Distinct domains of the spinal muscular atrophy protein SMN are required for targeting to Cajal bodies in mammalian cells.

Benoît Renvoisé, Kevinee Khoobarry, Marie-Claude Gendron, Christian Cibert, Louis Viollet, Suzie Lefebvre

This manuscript has been accepted for publication in Journal of Cell Science 119: 680-692 doi: 10.1242/jcs.02782

Distinct domains of the spinal muscular atrophy protein SMN are required for targeting to Cajal bodies in mammalian cells

Benoît Renvoisé [1], Kevinee Khoobarry [1], Marie-Claude Gendron [2], Christian Cibert [3], Louis Viollet[4] and Suzie Lefebvre [1, 4]*

[1]Laboratoire de Biologie Cellulaire des Membranes, Institut Jacques Monod (IJM), UMR 7592 CNRS/Universités Paris 6 et 7, 2 Place Jussieu, 75251 Paris cedex 05, France

[2] Service de Cytométrie, IJM

[3]Laboratoire de Morphométrie et Modélisation Cellulaire, IJM

[4]UR393 INSERM, IRNEM Institute, Hôpital Necker-Enfants Malades, Paris, France

Words:

Running title: SMN localization in CBs

Key words: gems, Cajal bodies, Tudor domain, SMN, snRNPs, SMA

*To whom correspondence should be addressed:

Dr Suzie Lefebvre
Institut Jacques Monod, UMR 7592 CNRS/Universités 6 et 7
Department of Cell Biology
2 Place Jussieu
75251 Paris cedex 05,
France.
Tel + 33 1 44 27 69 40
Fax + 33 1 44 27 59 94

E-mail: lefebvre@ijm.jussieu.fr

Abstract

Mutations of the survival motor neuron gene SMN1 cause the inherited disease spinal muscular atrophy. The ubiquitous SMN protein facilitates the biogenesis of spliceosomal small nuclear ribonucleoproteins, snRNPs. The protein is detected in the cytoplasm, nucleoplasm and enriched with snRNPs in nuclear Cajal bodies. It is structurally divided at least into an amino-terminal region rich in basic amino acid residues, a central Tudor domain, a self-association tyrosine/glycine-box and an exon7-encoded carboxy-terminus. To examine the domains required for the intranuclear localization of SMN, we have used fluorescently tagged-protein mutants transiently overexpressed in mammalian cells. The basic amino acid residues direct nucleolar localization of SMN mutants. The Tudor domain promotes localization of proteins in the nucleus and it cooperates with the basic amino acid residues and the tyrosine/glycine-box for protein localization in Cajal bodies. Moreover, the most frequent disease-linked mutant SMN□ex7 reduces accumulation of snRNPs in Cajal bodies, suggesting that the C-terminus of SMN participates in targeting to Cajal bodies. A reduced number of Cajal bodies in patient fibroblasts associates with the absence of snRNPs in Cajal bodies, revealing that intranuclear snRNA organization is modified in disease. These results indicate that both direct and indirect mechanisms regulate localization of SMN in Cajal bodies.

Introduction

Proximal spinal muscular atrophy (SMA) is a group of autosomal recessive neuromuscular disorders with childhood onset characterized by motor neuron degeneration and progressive paralysis. The disease is caused by mutations of the gene encoding the survival motor neuron (SMN) protein, SMN1 (Lefebvre et al., 1995). SMN1 and its nearly identical copy, SMN2, are within duplications on chromosome 5q13. Compared to SMN1, SMN2 is unique in that a single nucleotide change generates alternative splicing of SMN2 exon 7 (ex7), resulting in replacement of the C-terminal 16 amino acids (aa) by a 4-aa sequence (SMNΔex7). Indeed, it has been demonstrated that this unique nucleotide is included in a splice enhancer (Hofmann et al., 2000; Cartegni et al., 2002) and/or a splice inhibitor site (Kashima and Manley, 2003). The identical full-length SMN1 and SMN2 transcripts produce the ubiquitous 38 kDa SMN protein (Liu and Dreyfuss, 1996; Coovert et al., 1997; Lefebvre et al., 1997). A close correlation exists between the reduced levels of the SMN protein and the severity of SMA disease (Coovert et al., 1997; Lefebvre et al., 1997). The level of SMN fluctuates considerably in different cell types and during development (Burlet et al., 1998; La Bella et al., 1998). This modulation appears to be a key to its function, since the integrity of nuclear bodies (NBs) could be disrupted after SMN depletion in SMA patients and mouse models (Schrank et al., 1997; Frugier et al., 2000; Hsieh-Li et al., 2000; DiDonato et al., 2001; Monani et al., 2003). Why SMN and SMNΔex7 isoforms exist remains unknown. It is recognized that they have different functional properties, such that SMNΔex7, which preponderates in SMA patients, does not fully compensate for the absence of SMN1 (Lefebvre et al., 1995). The mechanism by which SMN depletion induces the neuromuscular defect is still elusive.

The SMN protein localizes mostly in the cytoplasm and accumulates in nuclear bodies frequently overlapping with Cajal bodies (CBs), named gems (gemini of CBs; Liu and Dreyfuss, 1996). SMN is a component of a large multiprotein complex comprising gemin2 to 7, which participates in the assembly of proteins and RNAs (reviewed in Meister et al., 2002a; Gubitz et al., 2004). Particularly, it has been shown that SMN facilitates various steps of the biogenesis of the spliceosomal U snRNPs (Uridine-rich small nuclear ribonucleoproteins) that are part of the spliceosome essential for the removal of introns during pre-mRNA splicing. The biogenesis of snRNPs (U1, U2, U4 and U5) constitutes a complex pathway occurring in both the cytoplasm and nucleus (Will and Luhrmann, 2001). The SMN complex facilitates cytoplasmic assembly of spliceosomal Sm core proteins onto U snRNAs and recruitment of the snRNA cap hypermethylase (TGS1; Mouaikel et al., 2003), leading to the formation of

nuclear import-competent snRNPs. The SMN complex remains associated with the snRNPs along the entire cytoplasmic pathway (Massenet et al., 2002). In the nucleus, it appears that the CB-containing the SMN complex are the first sites of accumulation of newly imported snRNPs (Carvalho et al., 1999, Sleeman et al., 2001) and are involved in early nuclear stages of snRNA maturation (Jàdy et al., 2003).

SMN is encoded by eight exons generating a multidomain polypeptide of 294 aa (see Fig.2A). It contains the central Tudor domain flanked by a N-terminal lysine (K)-rich sequence and in the C-terminal region, by a proline (P)-rich, a tyrosine/glycine (YG)-box and the ex7 encoded domains. The Tudor domain, named because of its structural homology to repeats of the *Drosophila* tudor protein, is conserved among different RNA-binding proteins (Pontig, 1997; Selenko et al., 2001) and mediates SMN interaction with arginine-glycine (RG) motifs in several proteins (reviewed in Meister et al., 2002a; Gubitz et al., 2004), including the CB marker coilin and the Sm core proteins and their symmetrically dimethylated arginine (sDMA) isoforms (Friesen et al., 2001; Meister and Fischer., 2002b; Hebert et al., 2002; Boisvert et al., 2002). The K-rich sequence is embedded in the interspecies conserved RNA-binding domain (Lorson and Androphy, 1998a; Bertrandy et al., 1999). The P-rich domain associates with the actin-binding protein profilin (Giesemann et al., 1999). The YG-box domain is implicated in self-association in vitro (Lorson et al., 1998b) and a putative cytoplasmic retention signal is encoded by ex7 (Zhang et al., 2003).

Unravelling mechanisms by which a protein is localized to various subnuclear compartments is primordial to understand nuclear organization and human diseases (Phair and Misteli, 2000; Carmo-Fonseca et al., 2002; Bubulya and Spector, 2004; Zaidi et al., 2004). Thus far, no clear overview of the role of the SMN domains, particularly of the Tudor domain, in subnuclear localization exists (Mohaghegh et al., 1999; Le et al., 2000). The overexpressed SMA mutant SMN472□5 lacking the C-terminal half of SMN is localized throughout the nucleus (Lefebvre et al., 2002). Why SMN472□5 presents such a distribution has awaited further investigations. Here, we have systematically analysed the functional SMN domains and showed that they govern nucleocytoplasmic partition and intranuclear localization in the nucleoplasm, nucleoli and gems/CBs. The central Tudor domain cooperates with the YG-box and the K-rich sequence for the accumulation of SMN in CBs. The U snRNPs fail to concentrate in CBs of cells transiently transfected with the SMA mutant SMN□ex7, suggesting a role of the ex7 domain for the localization of U snRNPs in CBs. Furthermore, in fibroblasts of SMA patients there is no accumulation of snRNPs in NBs, indicating that SMN depletion affects the spatio-temporal distribution of snRNPs.

Materials and Methods

Engineered fluorescently tagged proteins

Full-length and SMN mutants were prepared by PCR-amplification from full-length human cDNA (Lefebvre et al., 1995), digested and subcloned into the appropriate restriction sites of the pEGFP vectors (Clontech). Subcloning the RT-PCR fragment from total RNA preparation of an SMA patient produced SMN ex7. Mutations were introduced in the GFP recombinants using the QuickChange mutagenesis kit (Stratagene). Oligonucleotides used for mutagenesis are available upon request. DNA sequencing and FP-immunoblotting confirmed the constructs.

Cell cultures and transfections

COS7, HeLa and human fibroblast cultures were maintained in DMEM supplemented with 10% FBS, penicillin (100 U/ml) and streptomycin (100 g/ml). Cells were plated in a 8-chamber culture Slide (Becton Dickson Lab.) and transfected with purified plasmid using FuGENE 6 (Roche Diagnostics) as described previously (Lefebvre et al., 2002).

Immunofluorescence and microscopy

At 16-48h post-transfection, COS and human cells were prepared for fluorescence microscopy (Lefebvre et al., 1997). The following antibodies were used: anti-TMG (mouse mAb at 1:4000, Calbiochem), anti-U2 snRNP-specific protein U2B" (4G3 mouse mAb at 1:200, ICN Pharmaceuticals), anti-coilin (mouse mAb at 1:125, Abcam or a kind gift from M. Carmo-Fonseca), anti-SMN (mouse mAb at 1:500, Trans Lab or 4B3 at 1:500, Burlet et al., 1998), purified rabbit anti-SMN peptide (1:500), secondary anti-rabbit and anti-mouse Cy3 (1:500, Jackson Laboratories) and anti-mouse Alexa 488 (1:500, Molecular Probes). Samples were incubated with 4,6-diamidino-2-phenylindole (DAPI, 0.1 g/ml), mounted in either AF1 (Cityfluor) or Mowiol (Hoechst) and observed by nonconfocal (Leica DMR, objective 63x/1,32) or confocal (LEICA TCS SP2 AOBS, objective 63x/1,32) microscopy. Nonconfocal images acquired with a cooled CCD camera (Micromax, Princetown Instruments, Inc.) using MetaView Imaging System were processed by ImageJ (rsb.info.nih.gov/ij) and prepared using Adobe photoshop.

Analysis of the fluorescence signals

Fluorescence images were acquired as a series (stack) of optical sections of 1 m along the

optical axis (z) of the entire cell using a on a confocal microscope (LEICA TCS SP2 AOBS). The sensitivity of the photomultiplier tube was adjusted so that the fluorescence signal of the FP-fusion proteins was below the saturation level. The monographies (512x512 pixels) of each optical section were captured as 8-bit grayscale images. A segmentation algorithm was used to define the 'objects' by applying a threshold to each of the z-sections (ImageJ). The same segmentation algorithm was applied to automatically define the nuclear region by DAPI staining of each z-section. The proportion of fluorescence within the nucleus was calculated using ImageJ and was expressed as the percentage of the total fluorescence contained in the entire stack of z-sections. Ten cells were randomly selected and examined for each construct. The results presented values obtained from independent experiments and the significance was determined using the non-parametric Mann-Whitney test.

Flow cytometry

Cell sorting was performed with an EPICS Elite - ESP flow cytometer (Beckman-Coulter) equipped with a 15 mw argon-ion laser emitting at 488 nm and collecting through a 520 $\pm$ 15 nm bandpass filter for eGFP measurements. Sort windows were set to include cells with correct scatter profile and positive eGFP fluorescence.

Co-immunoprecipitations

The anti-GFP (Clonetech), anti-TMG (Calbiochem) and normal antibodies (DAKO) were incubated overnight at 4°C with total protein lysates from transfected cells with RIPA buffer (50 mM Tris-HCl, pH 7.4, 150 mM NaCl, 1% NP40, 0.1% SDS) in presence of RNAsin (1 U/ml, Promega) and protease inhibitors, and bound to Dynabeads M-280 sheep anti-rabbit or anti-mouse IgG (Dynal) for 2 hr at 4°C (Lefebvre et al., 2002). After four washes in RIPA, the proteins were eluted in SDS loading sample buffer and resolved by SDS-PAGE.

Immunoblot analyses

The proteins resolved by SDS-PAGE were transferred to a PVDF membrane and incubated with antibodies directed against GFP (mouse mAb at 1:1000, Roche Diagnostics), SMN (mouse mAb at 1:1000, Transduction Laboratories), gemin2 (mouse mAb at 1:1000, Abcam), Sm proteins (Y12 mouse mAb at 1:500, Abcam) and □-tubulin (mouse mAb at 1:10000, Sigma). The membranes were incubated with horseradish peroxidase-conjugated secondary antibody and detected by chemiluminescence (Amersham).

Results

The fluorescently tagged SMN protein behaves like the endogenous SMN

The localization of transiently expressed fluorescently tagged (FP)-SMN in COS cells and immortalized Type I (severe) SMA fibroblasts was compared to the localization of the endogenous SMN (Fig. 1). Immunofluorescence microscopy showed that SMN localized in the cytoplasm and concentrated in NBs in COS cells as reported in HeLa cells (Fig. 1A, Liu and Dreyfuss, 1996). In immortalized Type I SMA fibroblasts containing residual levels of SMN (Lefebvre et al., 2002), SMN was detected in the cytoplasm, nucleoplasm and occasionally, in NBs (Fig. 1D). Each cell line was transfected with FP-SMN and the distribution of transfected and endogenous SMN was similar (Fig. 1B, E). To determine if SMN localizes in gems and/or CBs in COS cells, we examined the localization of the CB marker coilin and of the gems markers SMN and gemin2. Analyses of the localization of SMN and coilin foci showed that SMN and coilin colocalized in CBs (Fig. 1G) in over 71% of cells (n=704) and there were no nuclear foci in the remainder of cells. The SMN and gemin2 foci were completely colocalized (Fig. 1H) in 64% of cells (n=602). Further immunofluorescence studies showed that SMN and 2,2,7-trimethylguanosine (TMG)-capped snRNAs of snRNP foci were colocalized (Fig. 1I) in 35% of cells (n=105). In most cell types (Carvalho et al., 1999; Young et al., 2001a) and in COS cells, gems and CBs constituted the same nuclear substructure.

The Tudor domain is not sufficient for SMN localization in CBs

The RG-motif of coilin serves to recruit the SMN to CBs (Hebert et al., 2002), but the SMN Tudor domain interacts with the RG-motif of other proteins (reviewed in Terns and Terns, 2001; Meister et al., 2002a; Gubitz et al., 2004), and it seemed likely that localization in CBs might involve other regions of SMN. To test this hypothesis, we generated (Fig. 2A) and transiently overexpressed a series of fluorescently tagged SMN deletion mutants in COS cells. We chose the primate COS cells that do not have the SMN2 gene and consequently, do not express the SMNΔex7 transcript. The integrity of fusion proteins was first verified by immunoblotting analyses (Fig. 2B). Each construct expressed a protein at the expected position. Given the transfection efficiency, the levels of fusion proteins were comparable, except for ex2B, as judged by both anti-tubulin and anti-SMN incubations.

Protein localization in transfected COS cells was analysed by fluorescence microscopy (Fig. 2C). SMN protein was first divided into three fragments containing the N-terminal region FP-SMNN86 (aa 1-86, N86), the central Tudor domain FP-SMNTudor (aa 87-146,

Tudor) or the C-terminal region FP-SMNΔN189 (aa 190-294, ΔN189). All these failed to accumulate in nuclear foci, demonstrating that none of these regions alone contains sufficient information for targeting to NBs. Fragments N86 and Tudor accumulated in respectively nucleoli and irregularly shaped nuclear substructures resembling speckles, and ΔN189 was localized in the cytoplasm. These results indicated that the sequences necessary for localization in NBs encompassed more than one region covered by the deletions.

It was first possible to conclude that a combination of N86 and the Tudor domain contributed to the localization of the SMA mutant SMN472Δ5 (aa 1-146, 472Δ5) in NBs. This mutant also localizes in the nucleoplasm and nucleoli (Fig. 2C; Lefebvre et al., 2002). Previous studies have implicated protein self-association in the formation of NBs (Hebert et al., 2000). A self-association domain has been mapped to the region encoded by SMN exon2B (aa 52-91; Young et al., 2000). To explore the role of this domain in localization, the construct FP-SMNex2B (aa 52-86) was generated and overexpressed: no fluorescence signal was observed in NBs, the protein being nuclear and concentrated in nucleoli, as judged by DAPI staining (Supplemental Fig. S1). We performed further mutagenesis experiments to identify which residues of the N-terminal region were responsible for the accumulation of SMN472Δ5 in NBs. The SMNex2B contains a K-rich sequence reminiscent of a cryptic nucleolar localization signal (NoLS) in coilin (Hebert et al., 2000) and similar to a consensus sequence for K-dependent NoLS (Horke et al., 2004; Fig. 2D). In view of the functional links between nucleoli and CBs (reviewed in Gall, 2003), we substituted the basic residues by asparagine (N) in FP-SMN472Δ5M2 (^{71}NNNPANNNN^{79}, 472Δ5M2) and in FP-SMNN86M2 (N86M2). The two mutants were localized exclusively in the nucleoplasm (Fig. 2D), indicating a contribution of the Tudor and K-rich domains in targeting SMN to CBs.

To further address the role of self-association in the localization of SMN, we tested deletions of the C-terminal ex7 and YG-box regions, which are involved in self-association of SMN (Lorson et al., 1998a). FP-SMNΔex7 (consisting of aa 1-278 plus the first 4 aa from ex8, Δex7) localized in the cytoplasm, nucleoplasm and nuclear foci (Mohaghegh et al., 1999; Le et al., 2000). Additional deletion of the YG-box in FP-SMNΔC40 (aa 1-254, ΔC40) showed a diffuse cytoplasm with a few aggregates (Fig. 2C). The simplest interpretation for these aggregates would be that they are due to proline stretches at the C-terminus of the protein. In the nucleus, ΔC40 was detected exclusively in the nucleoplasm, as were SMNΔex6/7 (aa 1-278; Vyas et al., 2002) and FP-SMNN194 (aa 1-194, N194, Fig. 2C). These results suggest that proline stretches move N194 away from NBs when compared with

472□5 and that the self-association YG-box enhances the localization of SMN to NBs. To test this possibility, we generated FP-SMN□N86 (aa 87-294, □N86) that corresponds to the addition of the Tudor domain to the C-terminal region □N189. □N86 localized in the cytoplasm and in contrast with □N189, accumulated in NBs, indicating that the Tudor and YG-box domains cooperate to localize in NBs (Fig. 2C). In addition, □N86 showed large cytoplasmic aggregates (blobs), which were not observed by overexpression of full-length FP-SMN (Fig. 1B) under our experimental conditions. In other studies the FP-SMN was shown to form cytoplasmic aggregates upon high expression levels (Shpargel et al., 2003; Sleeman et al., 2003). To exclude the possibility that localization in NBs was mediated by endogenous SMN, immortalized type I SMA fibroblasts with almost no NBs (6% of cells) were transfected with SMN constructs (Figs 1E, S2: □ex7, 472□5 and Tudor shown only). Localization in NBs of SMN mutants appears independent of the levels of endogenous SMN, indicating that transfected proteins present intrinsic properties. Similar localization patterns were also obtained in transfected HeLa cells (Fig. S3).

The NBs formed by the SMN mutants in transfected COS cells were further examined by immunofluorescence labelling of CB marker coilin. Coilin-positive CBs were nuclear substructures present in cells expressing the SMN mutants (Fig. 3, Table 1). The nuclear foci in FP-SMN transfected cells showed complete colocalization of FP-SMN and coilin. The SMN mutant □ex7, 472□5 and □N86 also showed complete colocalization with coilin in nuclear foci and they can be considered as CBs. However, the number of coilin foci obtained with these mutants was greater than in FP-SMN transfected cells, which was comparable to the number of foci in untransfected cells (Fig. 1G). In contrast, the FP signal failed to accumulate in CBs of cells transfected with N86, Tudor, ex2B, □C40 or □N189 (Fig. 3). Our results indicate that overexpression of SMN deletion mutants does not interfere with the ability of CBs to accumulate coilin.

Multiple interacting motifs regulate the nucleocytoplasmic distribution of SMN

To further characterize the nucleocytoplasmic distribution of FP-fusion proteins, we examined the ratio of fluorescence intensity in the nucleus versus the whole cell by confocal microscopy (Fig. 4A). The heterogeneity in fluorescence partitioning of some constructs was possibly due to cytoplasmic signals outside the threshold range. The analyses revealed that □N86 and FP-SMN had similar nuclear proportion of fluorescence (Mann-Whitney test, *not significant* at P□5%), indicating that removal of the N-terminal region has no effect on

nucleocytoplasmic partitioning of SMN. The fraction of Δex7 associated with the nucleus was significantly increased compared to FP-SMN (*P*<5%). The nuclear fraction of ΔC40 was also increased compared to Δex7 (*P*<5%). These results indicate that efficient oligomerization mediated by the YG-box and ex7 domain contributes to the nucleocytoplasmic distribution of SMN. Additional removal of aa 147 to 194 encoded by exon 4 caused the increase of 472–5 in the nucleus compared to ΔC40 and N194 (*P*<5%). We then tested whether accumulation in CBs might influence the value of the nuclear fraction. 472–5 and 472–5M2 were similarly associated with the nucleus, indicating that CB accumulation was dispensable for nuclear localization. In addition, the nuclear fraction of both the Tudor and ex2B regions increased compared to the other SMN constructs (*P*<5%). To further assess their importance in nuclear localization of SMN, the ex2B and Tudor regions were independently fused to the cytoplasmic protein 14.3.3ζ conjugated to eGFP (Strochlic et al., 2004, Fig. 4B-D): only the Tudor domain contained information to localize the protein in the nucleus. This agrees with the observation that partial deletion of the ex2B region has no major effect on the nucleocytoplasmic distribution of SMN (Le et al., 2000). From these studies we concluded that SMN has no classical NLS and that nuclear accumulation is regulated positively by the Tudor domain and negatively by the C-terminal portion of SMN.

SnRNPs presence is not critical for the localization of SMN mutants in CBs

It has been shown that overexpression of SMNΔN27 lacking the first 27 N-terminal aa results in the redistribution of the snRNPs to enlarged cytoplasmic and nuclear structures (Pellizzoni et al., 1998). To extend these observations, we determined whether our SMN mutants localized in CBs due to the presence of snRNPs (Table 1, Fig. 5). The distribution of the TMG-capped snRNA of snRNPs was examined. The speckled nucleoplasmic distribution of TMG in transfected cells appeared similar to that of untransfected cells (Fig. 1I), indicating no striking effect of the transfected SMN mutants tested over the nucleoplasmic pool of snRNPs (Fig. 5A). TMG foci were detected in cells transfected with N86 and FP-SMN, as also in the untransfected cells (Fig. 1I), indicating that overexpression of fluorescently tagged-proteins per se does not affect the composition of CBs. In contrast, a great reduction in the number of transfected cells with TMG foci was observed upon the overexpression of Δex7, ΔN86 and 472–5 (*P*<21%). In those cells, the remainder of TMG foci coincided with the FP foci (Fig. 5A). Overexpression of the Tudor domain, which partially overlapped the nucleoplasmic snRNPs, also depleted snRNPs from CBs. Immunofluorescence experiments

using 4G3 monoclonal antibody against the U2 snRNP-specific B" protein confirmed that the number of snRNPs foci was reduced upon expression of these SMN mutants (Fig. 5B). In addition, mutant Δex7 led to the accumulation of TMG in CB in 30% of transfected HeLa cells (n=942, P<2.1%) compared to 55% and 60% with FP-SMN transfected (n=579) and untransfected (n=699) cells, respectively. These data indicate that Δex7 leads to reduction of snRNPs in CBs independently of cell type.

To assess the importance of the association of SMN with the snRNP Sm proteins on the localization in CBs, we tested the overexpression of FP-SMNE134K (E134K), a mutant harbouring a glutamic acid to lysine substitution at position 134 in Tudor domain. This mutation, which has been identified in a Type I SMA patient (Clermont et al., 1997), disrupts the in vitro binding of SMN to the Sm proteins, fibrillarin and GAR1 (Bülher et al., 1999; Whitehead et al., 2002). The E134K mutant was localized in the cytoplasm and concentrated in an increased number of nuclear foci (Fig. 5C; Mohaghegh et al., 1999). Some of the E134K foci colocalized with coilin in CBs in 52% of transfected cells and they were gems and CBs in the remainder of cells (Table 1). There were as many TMG foci in E134K-transfected cells as in untransfected cells, indicating that the E134K mutant did not affect the localization of snRNP in CBs probably because of its reduced ability to interact with Sm proteins (Buhler et al., 1999). Taken together with the observations that the other mutants tested depleted the snRNPs from CBs, these results indicate that SMA mutant E134K does not compete for SMN binding sites of snRNPs.

To further assess the role of SMN in the distribution of snRNP in CBs, we investigated the localization of the endogenous SMN in transfected COS cells (Table 1, Fig. 5D). Immunofluorescence analyses of the endogenous SMN was possible with N86, ΔN86, Tudor and 472–5 using an anti-SMN monoclonal antibody against either the N-terminus of SMN or a bacterially-expressed human SMNΔN86 (Burlet et al., 1998). Endogenous SMN accumulated in nuclear foci of cells transfected with N86, ΔN86 or Tudor, but no SMN foci were detected in 472–5-transfected cells (Fig. 5C; Table 1). These results indicate that the reduction of snRNPs in CBs is not associated with the absence of SMN in CBs.

Endogenous SMN protein associates with SMN mutants in transfected cells

Our results indicated that deletion of the C-terminus of SMN in SMNΔex7 significantly affects the localization of snRNPs in CBs. To investigate the consequences of ex7 deletion in transfected cells, the FP-SMN and FP-SMNΔex7 cell populations were

isolated and the levels of endogenous proteins examined. Immunoblot analyses of protein extracts from cells transfected with either construct revealed similar molar ratios of SMN, gemin2, SmB/B' and fusion proteins as compared to tubulin, indicating that there is no massive protein degradation upon transfection (Fig. 6A). Immunoprecipitation experiments performed using anti-GFP and anti-TMG antibodies showed that both FP-SMN and FP-SMN□ex7 are associated with endogenous SMN and gemin2 (Fig. 6B), and with snRNPs (Fig. 6C-D). Compared to FP-SMN, FP-SMN□ex7 displayed a different stoichiometry of the immunoprecipitated endogenous SMN and gemin2, suggesting that FP-SMN and FP-SMN□ex7 might not form the same complex. Association of FP-SMN□ex7 with endogenous SMN suggests that the depletion of snRNPs from CBs might be due to competitive binding of FP-SMN□ex7 with SMN complexes. Moreover, immunoprecipation experiments revealed that the SMN truncation mutants N86, 472□5 and □N86 associated with the endogenous SMN, indicating that they may affect the composition of the SMN complex (Fig. 6E-G). The Tudor domain did not immunoprecipitate the endogenous SMN, suggesting that deletion of the N- and C-terminal portions affects incorporation of the fusion protein into SMN complex (Fig. 6H).

SMA disease affects the distribution of snRNPs in CBs

To determine whether the levels of SMN influence the distribution of snRNPs in CBs, the intranuclear localization of SMN and TMG-capped snRNA of snRNPs was compared in immortalized fibroblasts derived from a control and a SMA Type I individual (Fig.7A). Double-labelling experiments showed complete colocalization of SMN and TMG foci in 40% of control fibroblasts, SMN foci did not accumulate snRNPs in 10% of cells and the remainder 50% of cells were devoid of nuclear foci (n= 953). In immortalized SMA Type I fibroblasts, SMN foci were observed in 6% of cells and these foci did not accumulate TMG (n=870). These results suggest that SMA patients mislocalize snRNPs. To determine whether the intranuclear localization of SMN and snRNPs was correlated with phenotypic severity, we examined the colocalization of SMN and TMG in NBs of sub-confluent primary skin fibroblasts derived from children affected with Type I (severe), Type II (intermediate) and Type III (moderate) SMA and a control infant (Fig. 7B-C). Immunofluorescence analyses showed that in 72% of fibroblasts (n=2037) from a control infant, SMN concentrated in nuclear foci. The SMN and coilin foci showed complete colocalization in CBs in 20% of control fibroblasts (n=600). The remaining 52% of cells were devoid of coilin foci, indicating

that the SMN foci were gems. The SMN and TMG foci showed complete colocalization in 10% of cells (n=1437). The remaining 62% of cells were devoid of TMG foci, indicating that some of the SMN/coilin foci must be devoid of TMG. The SMA-derived fibroblasts from Type I (n=913), II (n=1070) and III (n=1069) showed SMN foci in 6, 15 and 20% of cells, respectively. The SMA patients had a fewer SMN foci and the disease severity correlated with the number of cells with foci (Coovert et al., 1997). The SMN and coilin foci showed complete colocalization in SMA-derived fibroblasts from Type I (n=300), II (n=300) and III (n=200), indicating that the number of gems/CBs is correlated with disease severity. In all three types of SMA cells SMN foci did not accumulate TMG, indicating that defective snRNP distribution in CBs associates with the SMA disease.

Immortalized Type I SMA fibroblasts were transiently transfected with the expression vector encoding the FP-SMN and analysed using antibodies to coilin and TMG of snRNA. In both transfected (n=203) and non-transfected cells (n=200), coilin localized to nuclear foci in 82% of cells, suggesting that overexpression of FP-SMN does not enhance the formation of CBs (Sleeman et al., 2001). Cells expressing FP-SMN showed coilin and FP-SMN both concentrated in CBs (Fig. S2). The FP-SMN-positive NBs accumulated snRNPs in 26% of transfected cells (n=201). Consequently, transient expression of FP-SMN in SMA cells expressing reduced levels of endogenous SMN is sufficient to trigger accumulation of snRNPs in NBs.

Discussion

In this study we have analysed the accumulation of the SMA gene product SMN in the nuclear substructures gems and CBs using a series of fluorescent protein-tagged SMN mutants. Domains governing the nuclear and intranuclear localization of SMN have been identified. Furthermore, newly assembled spliceosomal snRNPs re-entering the nucleus associate with SMN (Narayanan et al., 2004) and transiently move into CBs (Sleeman et al., 2001). The role of CBs in snRNP maturation steps (Jàdy et al., 2003; Nesic et al., 2004) and in regeneration of snRNPs after splicing has been described (Pellizzoni et al., 1998; Stanek and Neugebauer, 2004; Schaffert et al., 2004). To better understand the nuclear roles of SMN, the localization of snRNPs in CBs of cells expressing SMN constructs was investigated. Cells transfected with SMA mutants show severe reduction of snRNPs in CBs whereas snRNPs accumulate in CBs of FP-SMN transfected cells. Moreover, in all three types of SMA-derived fibroblasts the capacity to accumulate snRNPs in CBs is abrogated.

Tudor and self-oligomerization YG-box domains regulate the nucleocytoplasmic distribution of SMN

The SMN Tudor domain is the prototype of a conserved structural motif found in nucleic acid-binding proteins (Selenko et al., 2001; Maurer-Stroh et al., 2003). This domain mediates interactions with a protein motif formed of RG-rich repeats. Moreover, sDMA residues in the RG-rich C-terminus of snRNP core Sm proteins increases its association to SMN (reviewed in Meister et al., 2002a; Gubitz et al., 2004). Recent studies have demonstrated that sDMA-containing proteins are localized in the nucleus (Boisvert et al., 2002) and several of these interact with the Tudor domain of SMN (Côté and Richard, 2005). Although the Tudor domain does not contain a classical NLS, we now report that it localizes a cytoplasmic protein to the nucleus and enhances the nuclear pool of SMA mutant 472□5 compared to N86 that lacks the Tudor domain. Following the current model, Tudor domain-containing SMN proteins enter the nucleus bound to snRNP Sm proteins and to factors of the snRNP nucleocytoplasmic trafficking machineries (Buhler et al., 1999; Massenet et al., 2002; Narayanan et al., 2004). Other examples of proteins co-imported into the nucleus exist, such as the arginine/serine (RS)-rich splicing factors (Cacéres et al., 1997), the U2 snRNP-specific U2B'' protein (Kambach and Mattaj, 1994) and the splicing factor SF3a (Nesic et al., 2004).

The role of the Tudor domain in nuclear localization is consistent with the abrogation of in vitro import of SMN after immunodepletion of snRNPs or deletion of the Sm-binding

Tudor domain, Δex3 (Narayanan et al., 2004). Our finding that deletion of the self-oligomerization YG-box (ΔC40) enhances nuclear localization as compared to Δex7 is somewhat unexpected, since mutations within the YG-box interfere with SMN-binding to Sm proteins (Pellizzoni et al., 1999; Wang and Dreyfuss, 2001) and deletion of this domain (Δex6) abrogates SMN import in vitro (Narayanan et al., 2004). However, nuclear localization of ΔC40 is consistent with the ability of the Tudor domain to interact in vitro with the general import factor importin-β in the context of Δex6 (Narayanan et al., 2004). Taken together, these results support the view that Tudor and self-oligomerization YG-box modulate nucleocytoplasmic partitioning of SMN.

Moreover, the finding that removal of the Tudor domain in ΔN189 does not diminish the nuclear fraction as compared with ΔN86, suggests that other mechanisms play a role in the nuclear localization of SMN proteins. Indeed, the association of the C-terminus of SMN with the zinc finger protein ZPR1 might regulate nuclear partitioning of SMN (Gangwani et al., 2005). If SMN can enter the nucleus only with the snRNPs, our results suggest the existence of different pathways for snRNP import, as previously postulated (Fischer et al., 1991).

Cooperation between domains regulates the localization of SMN in CBs

Our finding that the Tudor domain is essential but not sufficient for the localization of SMN proteins in CBs is somewhat unexpected, since it interacts directly with coilin and Sm proteins that both concentrate in CBs (Carmo-Fonseca et al., 1992). However, this is consistent with FRET (fluorescence resonance energy transfer) analyses that demonstrated the self-association of SMN in CBs of living cells (Dundr et al., 2004). Indeed, we find that the C-terminal YG-box stabilizes the localization of SMN in CBs. One explanation for the role of the YG-box in CB localization is that self-oligomerization may enhance SMN accumulation in CBs by promoting binding to CB components, such as snRNPs (Fischer et al., 1997; Liu et al., 1997; Pellizzoni et al., 2001; Wang and Dreyfuss, 2001). Moreover, we show that the K-rich region encoded by ex2B cooperates with the Tudor domain to accumulate SMN mutants in CBs. This domain possibly stabilizes the interaction of the Tudor domain with coilin as suggested by in vitro binding studies (Hebert et al., 2002). Other examples of proteins that employ different protein motifs for accumulation in CBs are the transcription elongation factor TFIIS (Smith et al., 2003), the nucleolar protein Nopp140 (Isaac et al., 1998) and the U4/U6 snRNP assembly factor SART3/p110 (Stanèk et al., 2004). This supports the view that nucleolar and CB components can promote on their own assembly of supramolecular nuclear

substructures (Misteli, 2001). Moreover, proteins that transiently accumulate in dynamic nuclear substructures may serve as molecular scaffold to concentrate nuclear factors (reviewed in Dundr and Misteli, 2001).

Additionally, overexpression of SMN mutants lacking at least the C-terminal half of SMN results in nucleolar accumulation of mutants. It has been reported that SMN fractionates with nucleolar proteins in cell cultures (Whitehead et al., 2002) and concentrates in nucleoli of some neuronal cell populations (Francis et al., 1998; Young et al., 2001a). Although, there is no nucleolar targeting signal (Andersen et al., 2005), K-rich sequences can direct a subset of proteins to the nucleolus (Schmidt-Zachmann and Nigg, 1993; Hebert and Matera, 2000; Horke et al., 2004). We have identified by mutagenesis that a K-rich sequence encoded by ex2B is required for the nucleolar accumulation of truncated SMN proteins. Furthermore, the functional relevance of this domain has been suggested by a number of molecular interactions (Young et al., 2000; Campbell et al., 2000; Charroux et al., 2000; Young et al., 2001b; Claus et al., 2004). Although nucleolar localization of SMN is still debated, snRNAs and snRNP subunits have been shown to accumulate in CBs and nucleoli (Carmo-Fonseca et al., 1992; Leung and Lamond, 2002; Gerbi et al., 2003; Sleeman et al., 2001; Andersen et al., 2005) and therefore, SMN might be found in nucleoli associated with snRNPs.

Defects of snRNP localization in CBs correlates with SMA disease

At the cellular level, decrease of SMN levels in SMA is reflected by a decrease in the accumulation of SMN in NBs (Fig. 6; Coovert et al., 1997; Lefebvre et al., 1997; Frugier et al., 2000). This implies that SMA could have consequences on the localization of snRNP in NBs. Here, we observed that the residual SMN-positive NBs fail to accumulate snRNPs in fibroblasts derived from patients of all three SMA types. This is consistent with the reduction of snRNP assembly in vitro observed using extracts from fibroblast cells of SMA patients (Wan et al., 2005). In addition, double heterozygous mice deficient in *Smn* and *Gemin2* showed reduced levels of assembled snRNPs (Jablonska et al., 2002). Therefore, other components involved in snRNP biogenesis might be either deficient or mislocalized in SMA cells. Upon transient expression of FP-SMN in immortalized SMA Type I fibroblasts, we observed that FP-SMN accumulates together with snRNPs in NBs, suggesting that mislocalization rather than absence of factors may be associated with the SMA phenotype.

Our analyses of the SMA-linked E134K mutant revealed that this mutation is partially defective in accumulation in coilin-positive CBs compared to FP-SMN and other SMA mutants such as ex7 and 472 5 that are concentrated in CBs (Table 1). The observation that

E134K was concentrated in gems rather than in CBs supports the idea that gems and CBs are distinct subnuclear structures and that defects in exchange between different classes of NBs might underlie SMA pathogenesis in a subpopulation of patients. Moreover SMN-containing gems, which are devoid of coilin, are usually not observed within nuclei of cells actively importing new snRNPs, suggesting that overexpression of E134K might interfere with snRNP import (Narayanan et al., 2004). Therefore, the complete colocalization of E134K and snRNPs in CBs suggests a more complex association of SMN with snRNPs in the nucleus and leaves open the question how this SMA mutation alters the biogenesis of snRNPs.

Transient expression of the SMN deletion mutants leads to depletion of snRNPs from CBs similar to what is observed in SMA cells. Although coilin is required for snRNP recruitment in CBs (Tucker et al., 2001; Hebert et al., 2001), it does not appear sufficient for the accumulation of snRNPs in CBs of cells transfected with our mutants. This is consistent with the idea that coilin does not regulate the dynamics of association with CBs of its components (Platani et al., 2002; Dundr et al., 2004). Moreover, the reduction of snRNPs in CBs of cells transfected with SMN□ex7, the most frequent SMA mutation, suggests that ex7 region is important for localization of snRNPs in CBs. This is inline with the following observations. Deletion of the SMN C-terminus encoded by ex7 diminishes the oligomerization of SMN (Lorson et al., 1998a) and its binding capacity for the Sm proteins (Pellizzoni et al., 1999; Wang and Dreyfuss, 2001) and for TGS1 (Mouaikel et al., 2003). Hypermethylation of the snRNA cap structure allows efficient nuclear migration of snRNPs (Mattaj, 1988; Fischer et al., 1991) and in turn, their passage through CBs (reviewed in Cioce and Lamond, 2005). In light of the presence of some mutants in CBs that are devoid of snRNPs, it is rather SMN that retains snRNPs in CBs than snRNPs that retain SMN proteins in CBs (Carvalho et al., 1999; Sleeman et al., 2001).

The exact stoichiometry of the individual components of the SMN complex has not been established (Carissimi et al., 2005). It is possible that the effects in the distribution of snRNPs in CBs observed as a result of expression of the SMN mutants can be accounted for by altered stoichiometry of the SMN complex. In the co-immunoprecipitation experiments FP-SMN and FP-SMN□ex7 associate with endogenous SMN and gemin2 in a distinct stoichiometry. This is in agreement with the idea that truncated SMN might form partially functional SMN complex in a dose-dependent manner. Indeed, truncated proteins rescue cell lethality in avian cell system (Wang and Dreyfuss, 2001) and partially restore neuromuscular functions in fruitfly larvae (Chan et al., 2003) and SMA mouse models (Le et al., 2005). Full-length SMN might possibly gain functionality within complexes containing the mutants,

suggesting that stabilization of SMN complexes could constitute potential therapeutics for SMA.

The typical distribution of coilin in 2 to 8 CBs was observed upon overexpression of FP-SMN, E143K, N86 and ΔC40 (Fig. 3). The number of CBs is enhanced with SMN mutants consisting of Tudor domain with deletion of the N-terminal and/or C-terminal regions, except with ΔC40. This observation suggests that ΔC40 does not affect the interaction of coilin with CBs. Unexpectedly, deletion of the YG-box self-oligomerization domain suppresses the effects of the deleted ex7 domain, indicating a functional link between these two domains. A detailed mutagenic analysis of coilin showed that mutations of putative phosphorylation sites resulted in similarly numerous CBs (Shpargel et al., 2003). The serine/threonine phosphatase 4 (Carnegie et al., 2003) interacts with the SMN complex and may regulate post-translational modifications of coilin and in turn, the formation of CBs.

In summary, we have shown that the Tudor domain plays a role in nuclear localization of SMN and its residency in CBs by a mechanism that does require binding of additional SMN motifs. In cells of SMA patients the remaining NBs are depleted of snRNPs, which could induce by the expression of the most frequent SMA mutant SMNΔex7. The possibility of mimicking the SMA defect in a cell model is a step towards molecular characterization of normal and pathological processes in vivo. Of additional interest, are the mislocalization of β-actin mRNP in a SMA mouse model (Rossoll et al., 2003) and the lack of RNA-binding proteins in tissues of SMA patients (Anderson et al., 2004). Thus, it has become apparent that SMN is involved in supramolecular structuring of the nucleus and aberrant spatial organization of ribonucleoprotein complexes might participate in SMA physiopathology.

Acknowledgements

We thank E. Bertrand (IGM-CNRS, Montpellier, France) and B. Séraphin (CGM-CNRS, Gif-sur-Yvette, France) for stimulating discussions, J. Cartaud and D. Paulin for the constant support and colleagues for critical reading of manuscript. We are grateful to M. Carmo-Fonseca, C. Dargemont, G. Dreyfuss and I. Mattaj for generously providing antibodies and L. Strochlic for GFP-14.3.3 This study was supported by INSERM, CNRS, Association Française contre les Myopathies and Andrew's Buddies (USA). BR is recipient of an undergraduate fellowship from Ministère de l'Education Nationale, de la Recherche et de la Technologie.

References

Anderson, K. N., Baban, D., Oliver, P. L., Potter A. and Davies, K. E. (2004). Expression profiling in spinal muscular atrophy reveals an RNA binding protein deficit. *Neuro*. *Disorders* **14**, 711-722.

Andersen, J.S., Lam Y.W., Leung A.K., Ong, S.E., Lyon, C.E., Lamond, A.I. and Mann, M. (2005). Nucleolar proteome dynamics. *Nature* **433,** 77-83.

Bertrandy, S., Burlet, P., Clermont, O., Huber, C., Fondrat, C., Thierry-Mieg, D., Munnich, A. and Lefebvre, S. (1999). The RNA-binding properties of SMN: Deletion analysis of zebrafish orthologue defines domains conserved in evolution. *Hum. Mol. Genet*. **8,** 775-782.

Boisvert, F. M., Côté, J., Boulanger, M. C., Cléroux, P., Bachand, F., Autexier, C. and Richard, S. (2002). Symmetrical dimethylarginine metylation is required for the localization of SMN in Cajal bodies and pre-mRNA splicing. *J. Cell Biol.* **159**, 957-969.

Bubulya, P. A. and Spector, D. L. (2004). On the move ments of nuclear components in living cells. *Exp. Cell Res.* **296**, 4-11.

Buhler, D., Raker, V., Luhrmann, R. and Fischer, U. (1999). Essential role for the Tudor domain of SMN in spliceosomal U snRNP assembly: implications for spinal muscular atrophy. *Hum. Mol. Genet.* **8,** 2351-2357.

Burlet, P., Huber, C., Bertrandy, S., Ludosky, M.A., Zwaenepoel, I., Clermont, O., Roume, J., Delezoide, A.L., Cartaud, J., Munnich, A. and Lefebvre, S. (1998). The distribution of SMN protein complex in human fetal tissues and its alteration in Spinal Muscular atrophy. *Hum. Mol. Genet.* **7**, 1927-1933.

Càceres, J.F., Misteli, T., Screaton, G.R., Spector, D.L. and Krainer, A. (1997). Role of the modular domains of SR proteins in subnclear localization and alternative splicing specificity. *J. Cell Biol.* **138**, 225-238.

Campbell, L., Hunter, K.M., Mohaghegh, P., Tinsley, J.M., Brasch, M.A. and Davies, K.E. (2000). Direct interaction of Smn with dp103, a putative RNA helicase: a role for Smn in transcription regulation? *Hum. Mol. Genet.* **9**, 1093-1100.

Carissimi, C., Baccon, J., Straccia, M., Chiarella, P., Maiolica, A., Sawyer, A., Rappsilber, J. and Pellizzoni, L. (2005). Unrip is a component of SMN complexes active in snRNP assembly. *FEBS Let.* **579**, 2348-2354.

Carmo-Fonseca, M., Pepperkok, R., Carvalho, M.T. and Lamond, A.I. (1992). Transcription-dependent colocalization of the U1, U2, U4/U6, and U5 snRNPs in coiled bodies. *J. Cell Biol.* **117**, 1-14.

Carmo-Fonseca, M., Platani, M. and Swedlow, J.R. (2002). Macromolecular mobility inside the cell nucleus. *Trends Cell Biol*. **12**, 491-495.

Carnegie, G. K., Sleeman, J. E., Morrice, N., Hastie, C. J., Peggie, M. W., Philip, A., Lamond, A□I. and Cohen P. T. (2003). Protein phosphatase 4 interacts with the Survival of Motor Neurons complex and enhances the temporal localisation of snRNPs. *J. Cell Sci*. **116**, 1905-1913.

Cartegni, L. and Krainer, A. R. (2002). Disruption of an SF2/ASF-dependent exonic splicing enhancer in SMN2 causes spinal muscular atrophy in the absence of SMN1. *Nat. Genet.* **30**, 377-384.

Carvalho, T., Almeida, F., Calapez, A., Lafarga, M., Berciano, M. T. and Carmo-Fonseca, M. (1999). The spinal muscular atrophy disease gene product, SMN: A link between snRNP biogenesis and the Cajal (coiled) body. *J. Cell Biol.* **147**, 715-728.

Chan, Y. B., Miguel-Aliaga, I., Franks, C., Thomas, N., Trülzsch, B., Sattelle, D. B., Davies, K. E. and van den Heuvel, M. (2003). Neuromuscular defects in a *Drosophila* survival motor neuron gene mutant. *Hum. Mol. Genet.* **12**, 1367-1376.

Charroux, B., Pellizzoni, L., Perkinson, R. A., Yong, J., Shevchenko, A., Mann, M. and Dreyfuss, G. (2000). Gemin4. A novel component of the SMN complex that is found in both gems and nucleoli. *J. Cell Biol.* **148**, 1177-1186.

Claus, P., Bruns, A. F. and Grothe, C. (2004). Fibroblast growth factor-2 binds directly to the survival of motoneuron protein and is associated with small nuclear RNAs. *Biochem. J.* **384**, 559-565.

Clermont, O., Burlet, P., Cruaud, C., Bertrandy, S., Melki, J., Munnich, A., Lefebvre, S. (1997) Mutation analysis of the SMN gene in undeleted SMA patients. *Am. J. Hum. Genet.* **61**, A329.

Cioce, M. and Lamond, A. I. (2005). Cajal Bodies: A Long History of Discovery. *Annu. Rev. Cell. Dev. Biol*. Advance review published online May 16, 2005.

Coovert D. D., Le, T. T., McAndrew, P. E., Strasswimmer, J., Crawford, T. O., Mendell, J. R., Coulson, S. E., Androphy, E. J., Prior, T. W. and Burghes, A. H. (1997). The survival motor neuron protein in spinal muscular atrophy. *Hum. Mol. Genet.* **6**, 1205-1214.

Côté, J and Richard, S. (2005). Tudor domains bind symmetrical dimethylated arginines. *J Biol Chem*. **280**, 28476-28483. *Epub 2005 Jun 6*.

.

DiDonato, C. J., Lorson, C. L., De Repentigny, Y., Simard, L., Chartrand, C., Androphy, E. J. and Kothary, R. (2001). regulation of murine survival motor neuron (*Smn*) protein levels by modifying *Smn* exon 7 splicing. *Hum Mol Genet* **10**, 2727-2736.

Dundr, M. and Misteli, T. (2001). Functional architecture in the cell nucleus. *Biochem. J.* **356**, 297-310.

Dundr, M., Hebert, M. D., Karpova, T. S., Stanek, D., Xu, H., Shpargel, K. B., Meier,

U. T., Neugebauer, K. M., Matera, A. G. and Misteli, T. (2004). In vivo kinetics of Cajal body components. *J. Cell Biol.* **164**, 831-842.

Fischer, U., Darzynkiewicz, E., Tahara, S. M., Dathan, N. A., Lührmann, R. and Mattaj, I. W. (1991). Diversity in the signals required for nuclear accumulation of U SnRNPs and variety in the pathways of nuclear transport. *J. Cell Biol.* **113**, 705-714.

Fischer, U., Liu, Q. and Dreyfuss, G. (1997). The SMN-SIP1 complex has an essential role in spliceosomal snRNP biogenesis. *Cell* **90**, 1023-1029.

Francis, J. W., Sandrock, A. W., Bhide, P. G., Vonsattel, J. P. and Brown, R. H. Jr. (1998). Heterogeneity of subcellular localization and electrophoretic mobility of survival motor neuron (SMN) protein in mammalian neural cells and tissues. *Proc. Natl. Acad. Sci. U S A.* **95**, 6492-6497.

Friesen, W. J., Massenet, S., Paushkin, S., Wyce, A. and Dreyfuss, G. (2001). SMN, the product of the spinal muscular atrophy gene, binds preferentially to dimethylarginine-containing protein targets. *Mol. Cell* **7**, 1111-1117.

Frugier, T., Tiziano, F. D., Cifuentes-Diaz, C., Miniou, P., Roblot, N., Dierich, A., Le Meur, M. and Melki, J. (2000). Nuclear targeting defect of SMN lacking the C-terminus in a mouse model of spinal muscular atrophy. *Hum. Mol. Genet*. **9**, 849-858.

Gall, J. G. (2003). The centennial of the Cajal bodies. *Nat. Rev. Mol. Cell Biol.* **4**, 975-980.

Gangwani, L., Flavell, R. A. and Davis, R. J. (2005). ZPR1 is essential for survival and is required for localization of the survival motor neuron SMN protein to Cajal bodies. *Mol. Cell Biol.* **25**, 2744-2756.

Gerbi, S. A., Borovjagin, A. V., Odreman, F. E. and Lange, T. S. (2003). U4 snRNA nucleolar localization requires the NHPX/15.5-kD protein binding site but not Sm protein or U6 snRNA association. *J. Cell Biol.* **162,** 821-832.

Giesemann, T., Rathke-Hartlieb, S., Rothkegel, M., Bartsch, J. W., Buchmeier, S., Jockusch, B. M. and Jockusch, H. (1999). A role for polyproline motifs in the spinal muscular atrophy protein SMN. Profilins bind to and colocalize with smn in nuclear gems. *J. Biol. Chem.* **274**, 37908-37914.

Gubitz, A. K., Feng, W. and Dreyfuss, G. (2004). The SMN complex. *Exp. Cell Res.* **296**, 51-56.

Hebert, M. D. and Matera, A. G. (2000). Self-association of coilin reveals a common theme in nuclear body localization. *Mol. Biol. Cell.* **11**, 4159-4171.

Hebert, M. D., Shpargel, K. B., Ospina, J. K., Tucker, K. E. and Matera, A. G. (2002). Coilin methylation regulates nuclear body formation. *Dev. Cell* **3**, 329-337.

Hofmann, Y., Lorson, C. L., Stamm, S., Androphy, E. J. and Wirth, B. (2000). Htra2-beta 1 stimulates an exonic splicing enhancer and can restore full-length SMN expression to survival motor neuron 2 (SMN2). *Proc. Natl. Acad. Sci. USA* **97**, 9618-9623.

Horke, S., Reumann, K., Schweizer, M., Will, H. and Heise, T. (2004). Nuclear trafficking of La Protein depends on a newly identified nucleolar localization signal and the ability to bind RNA. *J. Biol. Chem.* **279**, 26563-26570.

Hsieh-Li, H. M., Chang, J. G., Jong, Y. J., Wu, M. H., Wang, N. M., Tsai, C. H. and Li, H. (2000). A mouse model for spinal muscular atrophy. *Nat. Genet*. **24**, 66-70.

Isaac, C., Yang, Y. and Meier, U. T. (1998). Nopp140 functions as a molecular link between the nucleolus and the Coiled Bodies. *J. Cell Biol.* **142**, 319-329.

Jablonka, S., Holtmann, B., Meister, G., Bandilla, M., Rossoll, W., Fischer, U. and Sendtner, M. (2002). Gene targeting of Gemin2 in mice reveals a correlation between defects in the biogenesis of U snRNPs and motoneuron cell death. *Proc Natl Acad Sci USA* **99**, 10126-10131.

Jàdy, B. E., Darzacq, X., Tucker, K. E., Matera, A. G., Bertrand, E. and Kiss, T. (2003). Modification of Sm small nuclear RNAs occurs in the nucleoplasmic Cajal body following import from the cytoplasm. *EMBO J.* **22**, 1878-1888.

Kambach, C. and Mattaj, I. (1994). Nuclear transport of the U2 snRNP-specific U2B'' protein is mediated by both direct and indirect signalling mechanisms. *J. Cell Science* **107**, 1807-1816.

Kashima, T. and Manley, J. L. (2003). A negative element in SMN2 exon 7 inhibits splicing in spinal muscular atrophy. *Nat. Genet.* **34**, 460-463.

La Bella, V., Cisterni, C., Salaun, D. and Pettmann, B. (1998). Survival motor neuron (SMN) protein in rat is expressed as different molecular forms and is developmentally regulated. *Eur. J. Neurosci.* **10**, 2913-2923.

Le, T. T., Coovert, D. D., Monani, U. R., Morris, G. E. and Burghes, A. H. (2000). The survival motor neuron (SMN) protein: effect of exon loss and mutation on protein localization. *Neurogenet.* **3**, 7-16.

Le, T. T., Pham, L. T., Butchbach, M. E. R., Zhang, H. L., Monani, U. R., Coovert, D. D., Gavrilina, T. O., Xing, L., Bassell, G. J. and Burghes, A. H. M. (2005). SMN□7, the major product of the centromeric survival motor neuron (SMN2) gene, extends survival in mice with spinal muscular atrophy and associates with full-length SMN. *Hum. Mol. Genet.* **14**, 845-857.

Lefebvre, S., Bürglen, L., Reboullet, S., Clermont, O., Burlet, P., Viollet, L., Benichou, B., Cruaud, C., Millasseau, P., Zeviani, M. et al. (1995). Identification and characterization of a spinal muscular atrophy-determining gene. *Cell* **80**, 155-165.

Lefebvre, S., Burlet, P., Liu, Q., Bertrandy, S., Clermont, O., Munnich, A., Dreyfuss, G. and Melki, J. (1997). Correlation between severity and SMN protein level in spinal muscular atrophy. *Nature Genet*. **16,** 265-269.

Lefebvre, S., Burlet, P., Viollet, L., Bertrandy, S., Huber, C., Belser, C. and Munnich, A. (2002). A novel association of SMN with two major non-ribosomal nucleolar proteins and its implication in spinal muscular atrophy. *Hum. Mol. Genet.* **11**, 1017-1027.

Leung, A. K. and Lamond, A. I. (2002). In vivo analysis of NHPX reveals a novel nucleolar localization pathway involving a transient accumulation in splicing speckles. *J. Cell Biol.* **157,** 615-629.

Liu, Q. and Dreyfuss, G. (1996). A novel nuclear structure containing the survival of motor neuron protein. *EMBO J* **15,** 3555-3565.

Liu, Q., Fischer, U., Wang, F. and Dreyfuss, G. (1997). The spinal muscular atrophy disease gene product, SMN, and its associated protein SIP1 are in a complex with spliceosomal snRNP proteins. *Cell* **90**, 1013-1021.

Lorson, C. L. and Androphy, E. J. (1998a). The domain encoded by exon 2 of the survival motor neuron protein mediates nucleic acid binding. *Hum. Mol. Genet.* **7**, 1269-1275.

Lorson, C. L., Strasswimmer, J., Yao, J. M., Baleja, J. D., Hahnen, E., Wirth, B., Le, T., Burghes, A. H. and Androphy, E. J. (1998b). SMN oligomerization defect correlates with spinal muscular atrophy severity. *Nat. Genet.* **19**, 63-66.

Maurer-Stroh, S., Dickens, N. J., Hughes-Davies, L., Kouzarides, T., Eisenhaber, F. and Ponting, C. P. (2003). The Tudor domain royal family : tudor, plant agenet, Chromo, PWWP, and MBT domains. *Trends Biochem. Sci.* **28**, 69-74.

Massenet, S., Pellizzoni, L., Paushkin, S., Mattaj, I. W. and Dreyfuss, G. (2002). The SMN complex is associated with snRNPs throughout their cytoplasmic assembly pathway. *Mol. Cell Biol.* **22**, 6533-6541.

Mattaj, I. (1988). UsnRNP assembly and transport. In *Structure and Function of Major and Minor Small Nuclear Ribonucleoprotein Particles*. (ed. M. L. Birnsteil), pp. 100-114. Berlin, Heidelberg, New York, Springer Verlag.

Meister, G., Eggert, C. and Fischer, U. (2002a). SMN-mediated assembly of RNPs: A complex story. *Trends Cell Biol.* **12**, 472-478.

Meister, G. and Fischer, U. (2002b). Assisted RNP assembly: SMN and PRMT5 complexes cooperate in the formation of spliceosomal UsnRNPs. *EMBO J.* **21**, 5853-5863.

Misteli T. (2001). The concept of self-organization in cellular architecture. *J. Cell Biol.* **155**, 181-185.

Mohaghegh, P., Rodrigues, N. R., Owen, N., Ponting, C. P., Le, T. T., Burghes, A. H. and Davies K. E. (1999). Analysis of mutations in the Tudor domain of the survival motor neuron protein SMN. *Eur. J. Hum. Genet.* **7**, 519-525.

Monani, U. R., Pastore, M. T., Gavrilina, T. O., Jablonka, S., Le, T. T., Andreassi, C., DiCocco, J. M., Lorson, C., Androphy, E. J., Sendtner, M., Podell, M. and Burghes, A. H. (2003). A transgene carrying an A2G missense mutation in the SMN gene

modulates phenotypic severity in mice with severe (type I) spinal muscular atrophy. *J. Cell Biol.* **160**, 41-52.

Mouaikel, J., Narayanan, U., Verheggen, C., Martera, A. G., Bertrand, E., Tazi, J. and Bordonné, R. (2003). Interaction between the snRNA cap hypermethylase and the spinal muscular atrophy protein, SMN. *EMBO Rep.* **4**, 616-622.

Narayanan, U., Achsel, T., Lührmann, R. and Matera, A. G. (2004). Coupled in vitro import of UsnRNPs and SMN, the spinal muscular atrophy protein. *Mol. Cell* **16**, 223-234.

Nesic, D., Tanackovic, G. and Krämer, A. (2004). A role for Cajal bodies in the final steps of U2 snRNP biogenesis. *J. Cell Science* **117**, 4423-4433.

Pellizzoni, L., Kataoka, N., Charroux, B. and Dreyfuss, G. (1998). A novel function for SMN, the spinal muscular atrophy disease gene product, in pre-mRNA splicing. *Cell* **95**, 615-624.

Pellizzoni, L., Charroux, B. and Dreyfuss, G. (1999). SMN mutants of spinal muscular atrophy patients are defective in binding to snRNP proteins. *Proc. Natl. Acad. Sci. USA.* **96**, 11167-11172.

Pellizzoni, L., Charroux, B., Rappsilber, J., Mann, M. and Dreyfuss, G. (2001). A functional interaction between the survival motor neuron complex and RNA polymerase II. *J. Cell Biol.* **152**, 75-85.

Phair, R. D. and Misteli, T. (2000). High mobility of proteins in the mammalian cell nucleus. *Nature* **404**, 604-609.

Platani, M., Goldberg, I., Lamond, A. I. and Swedlow, J. R. (2002). Cajal body dynamics and association with chromatin are ATP-dependent. *Nat. Cell Biol*. **4**, 502-508

Pontig, C. P. (1997). Tudor domains in proteins that interact with RNA. *Trends in Biochem. Sci.* **22**, 51-52.

Rossoll, W., Jablonka, S., Andreassi, C., Kroning, A. K., Karle, K., Monani, U. R., Sendtner, M. (2003). Smn, the spinal muscular atrophy-determining gene product, modulates axon growth and localization of beta-actin mRNA in growth cones of motoneurons. *J. Cell Biol.* **163**, 801-812.

Schaffert, N., Hossbach, M., Heintzmann, R., Achsel, T. and Luhrmann, R. (2004). RNAi knockdown of hPrp31 leads to an accumulation of U4/U6 di-snRNPs in Cajal bodies. *EMBO J.* **23**, 3000-3009.

Schmidt-Zachmann, M. S. and Nigg, E. A. (1993). Protein localization to the nucleolus: a search for targeting domains in nucleolin. *J. Cell Science* **105**, 799-806.

Schrank, B., Gotz, R., Gunnersen, J.M., Ure, J.M., Toyka, K. V., Smith, A. G. and Sendtner, M. (1997). Inactivation of the survival motor neuron gene, a candidate gene

for human spinal muscular atrophy, leads to massive cell death in early mouse embryos. *Proc. Natl. Acad. Sci.* USA **94**, 9920-9925.

Selenko, P., Sprangers, R., Stier, G., Bühler, D., Fischer, U. and Sattler, M. (2001). SMN Tudor domain structure and its interaction with Sm proteins. *Nature Struc. Biol.* **8**, 27-31.

Shpargel, K. B., Ospina, J. K., Tucker, K. E., Matera, A. G. and Hebert, M. D. (2003). Control of Cajal body number is mediated by the coilin C-terminus. *J. Cell Sci.* **116,** 303-312.

Sleeman, J. E., Ajuh, P. and Lamond, A. I. (2001). snRNP protein expression enhances the formation of Cajal bodies containing p80-coilin and SMN. *J. Cell Sci.* **114**, 4407-4419.

Sleeman, J. E., Trinkle-Mulcahy, L., Prescott, A. R, Ogg, S. C. and Lamond, A. I. (2003). Cajal body proteins SMN and Coilin show differential dynamic behaviour in vivo. *J. Cell Sci.* **116**, 2039-2050.

Smith, A. J., Ling, Y. and Morgan G. T. (2003). Subnuclear localization and Cajal body targeting of transcription elongation factor TFIIS in amphibian oocytes. *Mol. Biol. Cell*. **14**, 1255-1267.

Stanek, D. and Neugebauer, K. M. (2004). Detection of snRNP assembly intermediates in Cajal bodies by fluorescence resonance energy transfer. *J. Cell Biol.* **166,** 1015-1025.

Strochlic, L., Cartaud, A., Mejat, A., Grailhe, R., Schaeffer, L., Changeux, J. P. and Cartaud, J. (2004). 14-3-3 □ associates with muscle specific kinase and regulates synaptic gene transcription at vertebrate neuromuscular synapse. *Proc. Natl. Acad. Sci. USA* **101**, 18189-18194.

Terns, M. P. and Terns, R. M. (2001). Macromolecular complexes: SMN-master assembler. *Curr. Biol.* **11**, R862-R864.

Tucker, K. E., Berciano, M. T., Jacobs, E. Y., LePage, D. F., Shpargel, K. B., Rossire, J. J., Chan, E. K., Lafarga, M., Conlon, R. A. and Matera, A. G.. (2001). Residual Cajal bodies in coilin knockout mice fail to recruit Sm snRNPs and SMN, the spinal muscular atrophy gene product. *J. Cell Biol.* **154**, 293-307.

Vyas, S., Bechade, C., Riveau, B., Downward, J. and Triller, A. (2002). Involvement of survival motor neuron (SMN) protein in cell death. *Hum. Mol. Genet.* **11**, 2751-2764.

Wan, L., Battle, D. J., Yong, J., Gubitz, A. K., Kolb, S. J., Wang, J., Dreyfuss, G. (2005). The survival of motor neurons protein determines the capacity for snRNP assembly: biochemical deficiency in spinal muscular atrophy. *Mol. Cell. Biol.* **25**, 5543-5551.

Wang, J. and Dreyfuss, G. (2001). A cell system with targeted disruption of the SMN gene : functional conservation of the SMN protein and dependence of gemin2 on SMN. *J. Biol. Chem.* **276**, 9599-9605.

Whitehead, S. E., Jones, K. W., Zhang, X., Cheng, X., Terns, R.M. and Terns, M. C. (2002). Determinants of the interaction of the spinal muscular atrophy disease protein SMN with the dimethylarginine-modified box H/ACA small nucleolar ribonucleoprotein GAR1. *J. Biol. Chem.* **277**, 48087-48093.

Will, C. L. and Luhrmann, R. (2001). Spliceosomal UsnRNP biogenesis, structure and function. *Curr. Opin. Cell. Biol.* **13**, 290-301.

Young, P. J., Man, N. T., Lorson, C. L., Le, T. T., Androphy, E. J., Burghes, A.H. and Morris, G.E. (2000). The exon 2b region of the spinal muscular atrophy protein, SMN, is involved in self-association and SIP1 binding. *Hum*. *Mol*. *Genet*. **9**, 2869-2877.

Young, P. J., Le, T. T., Dunckley, M., Nguyen, T. M., Burghes, A. H. and Morris, G. E. (2001a). Nuclear gems and Cajal (coiled) bodies in fetal tissues: nucleolar distribution of the spinal muscular atrophy protein, SMN. *Exp. Cell Res.* **265**, 252-261.

Young, P. J., Day, P. M., Zhou, J., Androphy, E. J., Morris, G. E. and Lorson, C. L. (2001b). A direct interaction between the survival motor neuron protein and p53 and its relationship to spinal muscular atrophy. *J. Biol. Chem.* **277**, 2852-2859.

Zaidi, S. K., Young, D. W., Choi, J. Y., Pratap, J., Javed, A., Montecino, M., Stein, J. L., Lian, J. B., van Wijnen, A. J. and Stein, G. S. (2004). Intranuclear trafficking: Organization and assembly of regulatory machinery for combinatorial biological control. *J*. *Biol*. *Chem*. **279**, 43363-43366.

Zhang, H. L., Pan, F., Hong, D., Shenoy, S. M., Singer, R. H. and Bassell, G. J. (2003). Active transport of the survival motor neuron protein and the role of exon-7 in cytoplasmic localization. *J. Neurosci.* **23**, 6627-6637.

Legends

Figure 1. Localization of the endogenous SMN and of FP-SMN in transfected cells. In both COS cells (A, B) and SMA type I fibroblasts (D, E), immunolocalization of the endogenous SMN (A, D) and direct detection of FP-SMN (B, E) revealed that the protein distributes to the cytoplasm, nucleoplasm and concentrates in CBs. The eGFP diffusely localized throughout the cells (C, F). COS cells were double-labelled for SMN (green) and CB marker coilin (G), gem marker gemin2 (H) and snRNP marker TMG (I, red), respectively. Inserts show SMN colocalized with coilin, gemin2 and snRNP in CBs. Scale bars, 3 μm.

Figure 2. Systematic analysis of protein domains in subcellular distribution of SMN in transfected cells**. A)** SMN is depicted with the K-rich, Tudor, P-rich, YG-box and ex7 encoded domains. SMN and deletion mutants were fused to the N-ter eGFP (FP). Overexpressed FPs localized in the nucleus within nucleoli (No), the nucleoplasm (Np) and/or CBs. Detection is presented as + or – for the presence or absence of protein. **B**) Immunoblot analyses with anti-GFP antibodies of lysates from COS cells transiently transfected with the indicated constructs revealed that SMN, Δex7, ΔC40, ΔN86, N194, 472Δ5, N86, SMNTudor, SMNex2B recombinants and eGFP showed a major band of apparent mobility of 70, 63, 61, 57, 56, 55, 43, 39, 36 and 28 kDa, respectively. The α-SMN and α-tubulin incubations served as loading control of and relative expression levels, respectively. The position of molecular weight standards is indicated. **C)** The distribution pattern of the indicated constructs transiently overexpressed in COS cells and analysed by fluorescence microscopy. Some FPs accumulated in NBs (arrows) and/or in nucleoli (arrow head). **D)** SMN contains a conserved interspecies K-rich sequence highlighted by open boxes (Bertrandy et al., 1999). This motif resembles the NoLS identified in proteins such as MDM2, ARF and coilin (Hebert et al., 2000) and corresponds to a NoLS "consensus" sequence (Horke et al., 2004). Mutagenesis of the K-rich sequence identified a cryptic NoLS in the N-terminal portion of SMN (SMNN86M2) and revealed a role in subnuclear localization of 472Δ5 (SMN472Δ5M2) in CBs and nucleoli. Scale bars, 3 μm.

Figure 3. Comparison of the localization of SMN proteins with the CB marker coilin. The constructs indicated were transiently transfected into COS cells. Overexpression of FP-SMN, Δex7, 472Δ5 and ΔN86 colocalized with coilin in CBs (red), while N86, ex2B, Tudor, ΔC40 and ΔN189 did not form nuclear foci and were excluded from CBs. The mutants N86 and

ex2B accumulated also in nucleoli (see Fig. S1). The microscope was focused on coilin-positive CBs. Inserts show FPs (left), coilin (middle) and merge (right). Scale bars, 3 μm.

Figure 4. Analysis of protein domains required for nuclear localization of SMN. **A)** The proportion of fluorescence in the nucleus relative to the total fluorescence contained in the entire stack of z-sections is presented to visualize the distribution of 10 cells for each construct. **B)** The 14.3.3ζ protein localized to the cytoplasm. The 14.3.3ζ fused to the SMN ex2B region is remained in the cytoplasm, whereas fusion to the SMN Tudor domain led to accumulation of the protein in the nucleus. Scale bars, 3 μm.

Figure 5. Accumulation of the endogenous SMN, coilin and snRNPs in CBs of COS cells transiently transfected with SMN constructs. **A)** Distribution of snRNPs in cells transfected with SMN mutants: SMN, SMNΔN86, SMNΔex7 and SMNTudor (green) were co-stained using anti-TMG snRNA antibodies (red). **B)** Cells transfected with SMN mutants (green) were immunolabelled for the endogenous SMN (red). **C)** Distribution of coilin, TMG and U2 snRNP- specific B" protein in COS cells transfected with SMNE134K mutants. **D)** Distribution of the U2 snRNP-specific B" protein in cells transiently transfected with SMN mutants. Inserts showed magnified distribution of those components in NBs of transfected cells. **E)** Analyses are also presented using histograms. Scale bars, 3 μm.

Figure 6. Analyses of the interaction of the fluorescently tagged SMN mutants with the endogenous SMN and snRNPs. **A)** COS cells were either transfected with the FP-SMN or FP-SMNΔex7. Immunoblotting shows no massive degradation of gem/CB components in whole-cell extracts prepared from FACS-selected cells. **B-H)** Cell extracts were subject to immunoprecipitation with anti-GFP (GFP IP) or anti-TMG snRNA antibodies (TMG IP) and analysed by immunoblotting for the endogenous SMN. Anti-GFP incubation served as loading control. SMN mutants co-immunoprecipated the endogenous SMN, except for the Tudor mutant. Both FP-SMN and FP-SMNΔex7 co-immunoprecipitated with anti-TMG antibodies as confirmed with control IgG (DAKO IP). Light (lig) and heavy chains of immunoglobulins (hig).

Figure 7. Subnuclear localization of coilin, SMN and TMG of snRNA in SMA-derived fibroblasts. **A)** Immortalized control and SMA Type I patient fibroblasts were costained for

SMN (green) and the snRNP marker TMG (red). SMN foci in control cells were colocalized with snRNPs, as shown in the insert. In contrast, SMN foci detected in SMA cells were never found positive for snRNP, as shown in the insert. It should be noted that coarsening of the TMG labelling in the nucleoplasm of SMA cells was also observed in controls. **B)** Primary fibroblasts derived from control and SMA Type I, II and III were immunostained for SMN (green) and coilin (red). **C)** Primary fibroblasts derived from control and SMA Type I, II and III were immunostained for SMN (green) and TMG (red). Inserts showed SMN (left), coilin or TMG (middle) and merge (right). Scale bars, 3 μm.

Figure S1. Presence of transiently expressed N86 and SMNex2B in the nucleoli (arrow head) of COS cells, as judged by DNA-staining with DAPI. Scale bars, 3 μm.

Figure S2. Distribution of mutant SMN Δex7 (**A**), 472Δ5 (**B**) and Tudor (**C**) observed under transient transfection of immortalized SMA Type I fibroblast cells expressing low levels of endogenous SMN. Immunolocalization of coilin in untransfected (D) and FP-SMN transfected (**E**) SMA cells. Immunolocalization of TMG in SMA cells transfected with FP-SMN (**F**). Inserts show FP-SMN (left), coilin or TMG (middle) and merge (right). Scale bars, 3 μm.

Figure S3. Immunolocalization of the endogenous SMN and localization of the indicated constructs transiently overexpressed in HeLa cells, and analysed by fluorescence microscopy. Scale bar, 3 μm.

Table 1. Analyses of CBs in transiently transfected COS cells with SMN mutants

	Proportion of cells with							
	P80-CB (%)	**P80-positive FP foci (%)**	**endogenous SMN foci (%)**	**endogenous SMN-positive FP foci (%)**	**TMG foci (%)**	**TMG-positive FP foci (%)**	**U2B" foci (%)**	**U2B"-positive FP foci (%)**
untransfected	**75 (n=717)**	**-**	**71 (n=704)**	**-**	**51 (n=205)**	**-**	**39 (n=200)**	**-**
Constructs[a]								
SMN*	**100 (n=79)**	**100**	**nd**	**nd**	**46 (n=100)**	**46**	**32 (n=412)**	**32**
SMNΔN86*	**95 (n=83)**	**100**	**88 (n=100)**	**88**	**9 (n=109)**	**9**	**5 (n=221)**	**5**
SMNΔex7*	**100 (n=132)**	**100**	**nd**	**-**	**5 (n=183)**	**5**	**6 (n=217)**	**6**
SMNΔC40	**80 (n=106)**	**-**	**nd**	**-**	**18 (n=228)**	**-**	**nd**	**-**
SMN-N194	**100 (n=56)**	**-**	**nd**	**-**	**11 (n=107)**	**-**	**nd**	**-**
SMN-Tudor	**100 (n=80)**	**-**	**34 (n=300)**	**-**	**12 (n=100)**	**-**	**nd**	**-**
SMN472Δ5*	**100 (n=61)**	**100**	**16 (n=108)**	**16**	**13 (n=100)**	**13**	**16 (n=189)**	**16**
SMN472Δ5M2	**80 (n=100)**	**-**	**nd**	**-**	**16 (n=100)**	**-**	**nd**	**-**
SMN-N86	**100 (n=101)**	**-**	**88 (n=172)**	**-**	**53 (n=406)**	**-**	**nd**	**-**
SMNE134K*	**76 (n=206)**	**52**	**nd**	**nd**	**58 (n=202)**	**54**	**41 (n=200)**	**41**

a, presented in the same order as in Fig. 2A.
***,** fusion proteins accumulated in CBs.
nd, not determined.

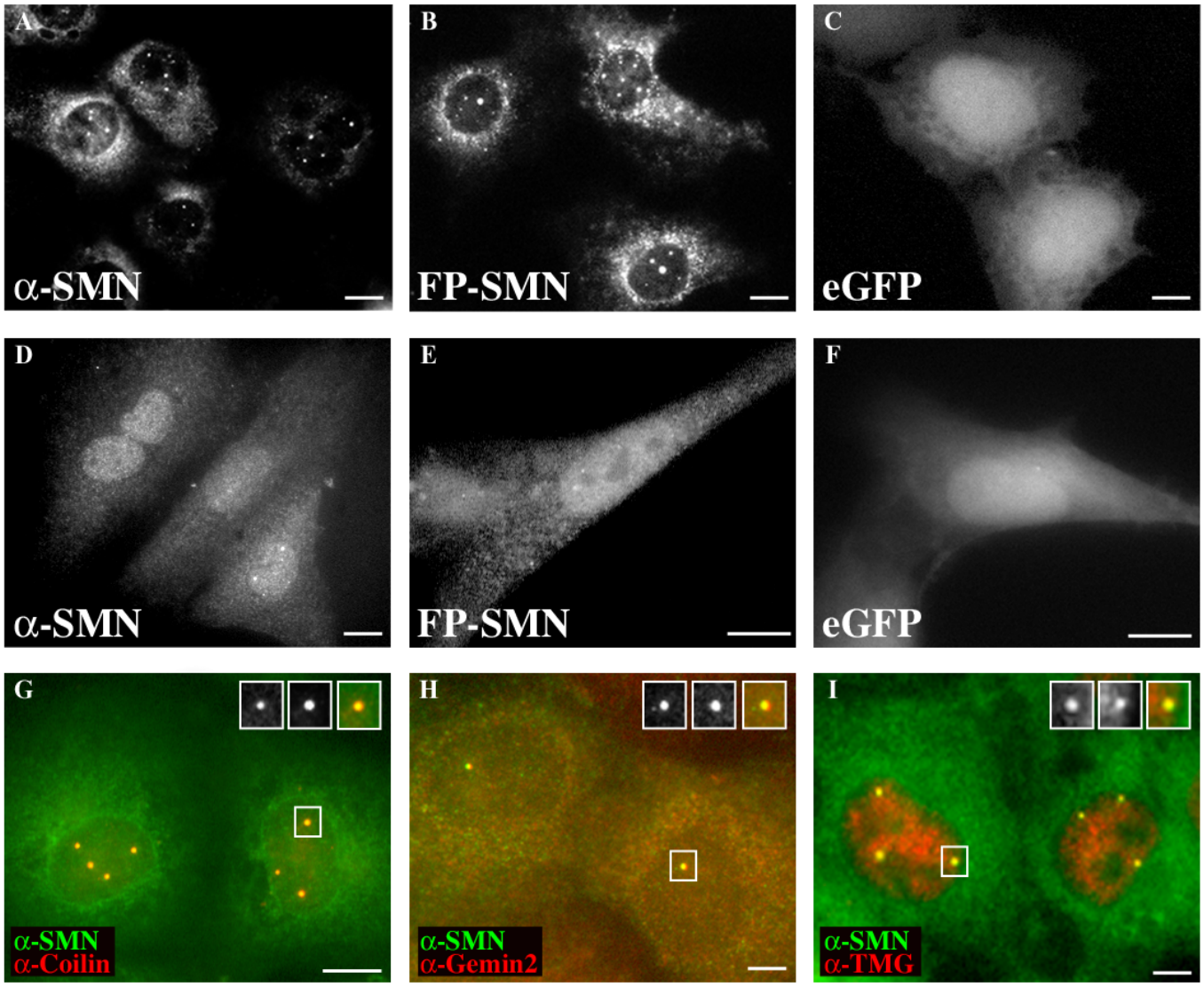
A
α-SMN
B
FP-SMN
C
eGFP
D
α-SMN
E
FP-SMN
F
eGFP
G
α-SMN
α-Coilin
H
α-SMN
α-Gemin2
I
α-SMN
α-TMG

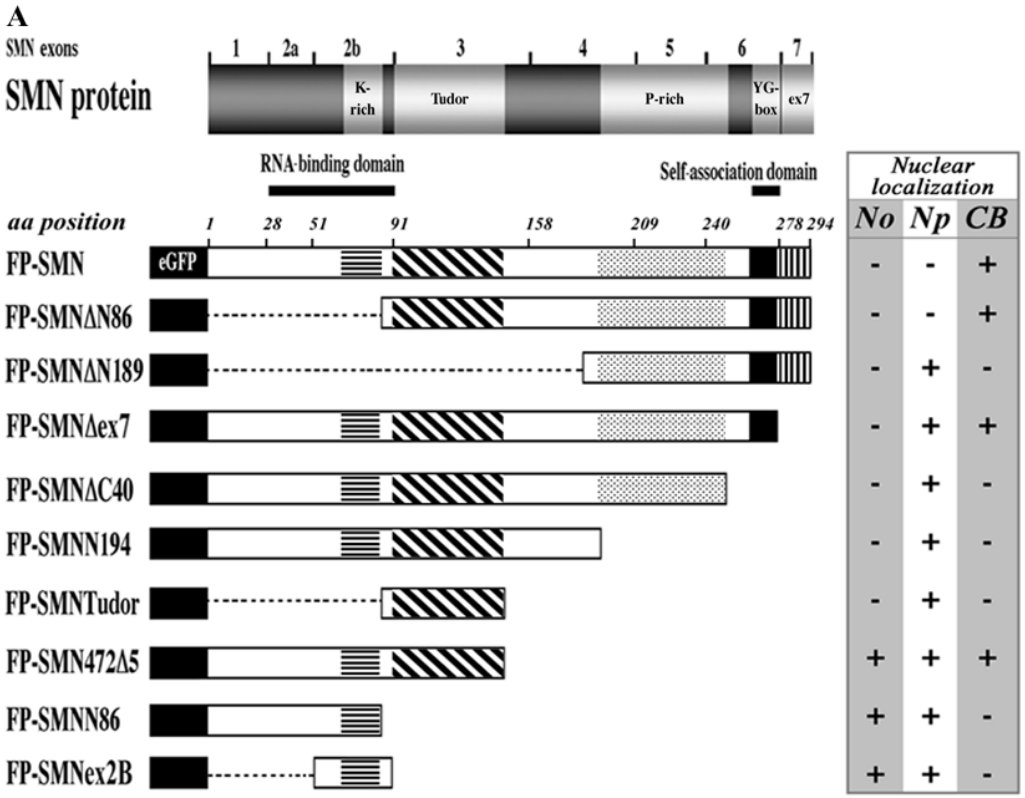
A
SMN exons
1 2a 2b 3 4 5 6 7
SMN protein
K-rich
Tudor
P-rich
YG-box
ex7
RNA-binding domain
Self-association domain
aa position
1 28 51 91 158 209 240 278 294
FP-SMN
FP-SMNΔN86
FP-SMNΔN189
FP-SMNΔex7
FP-SMNΔC40
FP-SMNN194
FP-SMNTudor
FP-SMN472Δ5
FP-SMNN86
FP-SMNex2B
eGFP
Nuclear localization
No Np CB
- - +
- - +
- + -
- + +
- + -
- + -
- + -
+ + +
+ + -
+ + -

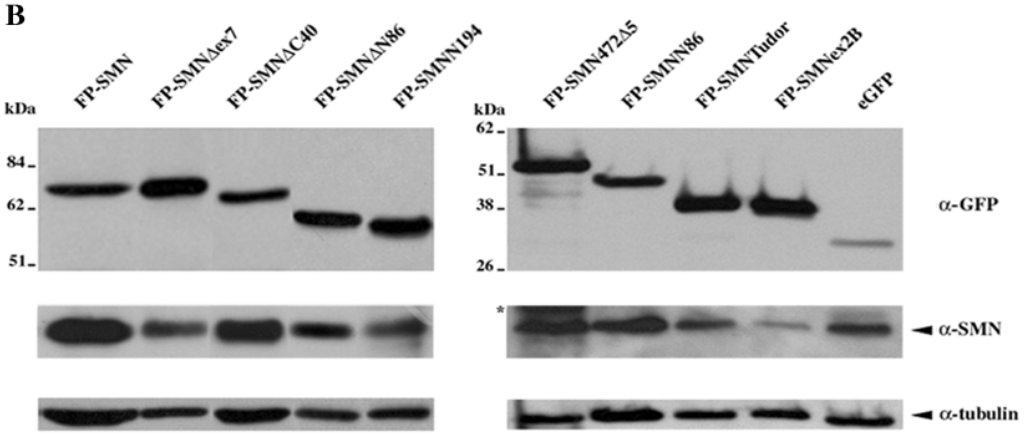
B
kDa
FP-SMN
FP-SMNΔex7
FP-SMNΔC40
FP-SMNΔN86
FP-SMNN194
84
62
51
FP-SMN472Δ5
FP-SMNN86
FP-SMNTudor
FP-SMNex2B
eGFP
62
51
38
26
α-GFP
α-SMN
α-tubulin

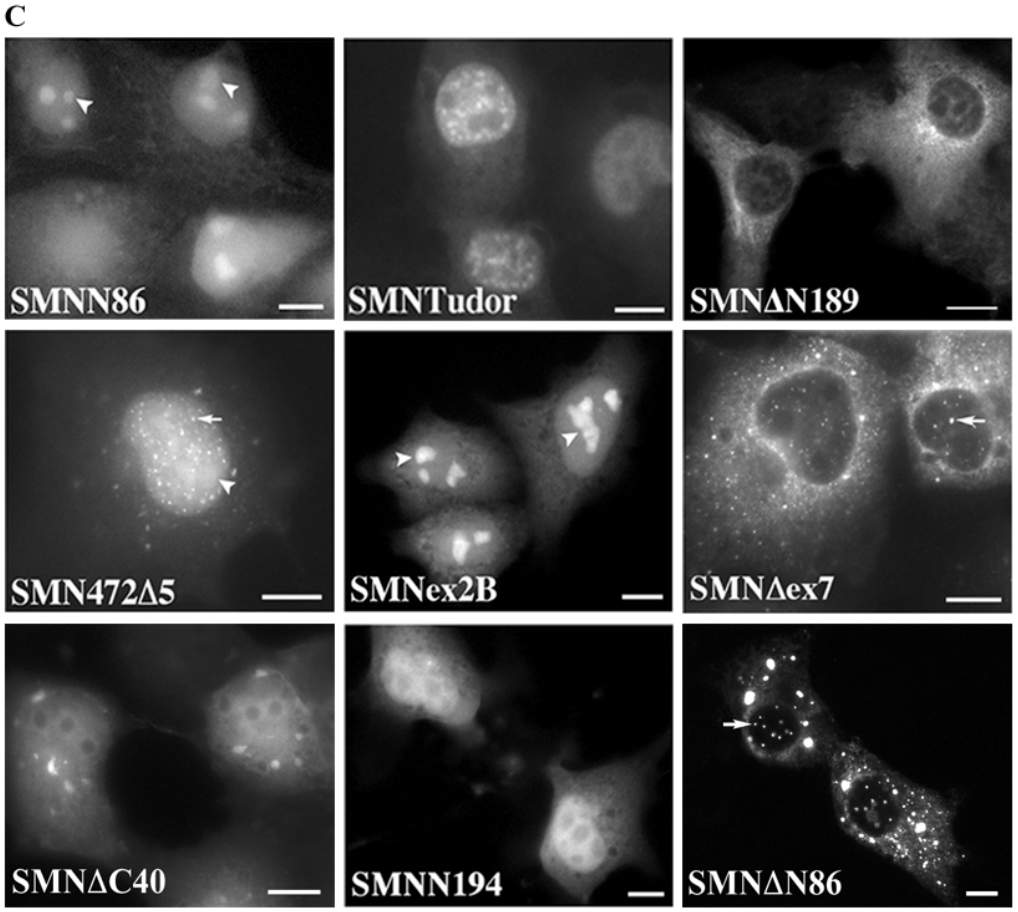
C
SMNN86
SMNTudor
SMNΔN189
SMN472Δ5
SMNex2B
SMNΔex7
SMNΔC40
SMNN194
SMNΔN86

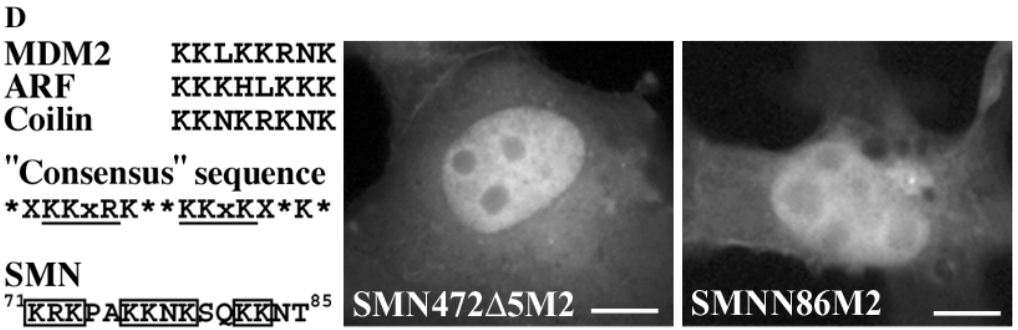
D
MDM2 KKLKKRNK
ARF KKKHLKKK
Coilin KKNKRKNK
"Consensus" sequence
*XKKxRK**KKxKX*K*
SMN
71 KRK P A KKNK S Q KK NT 85
SMN472Δ5M2
SMNN86M2

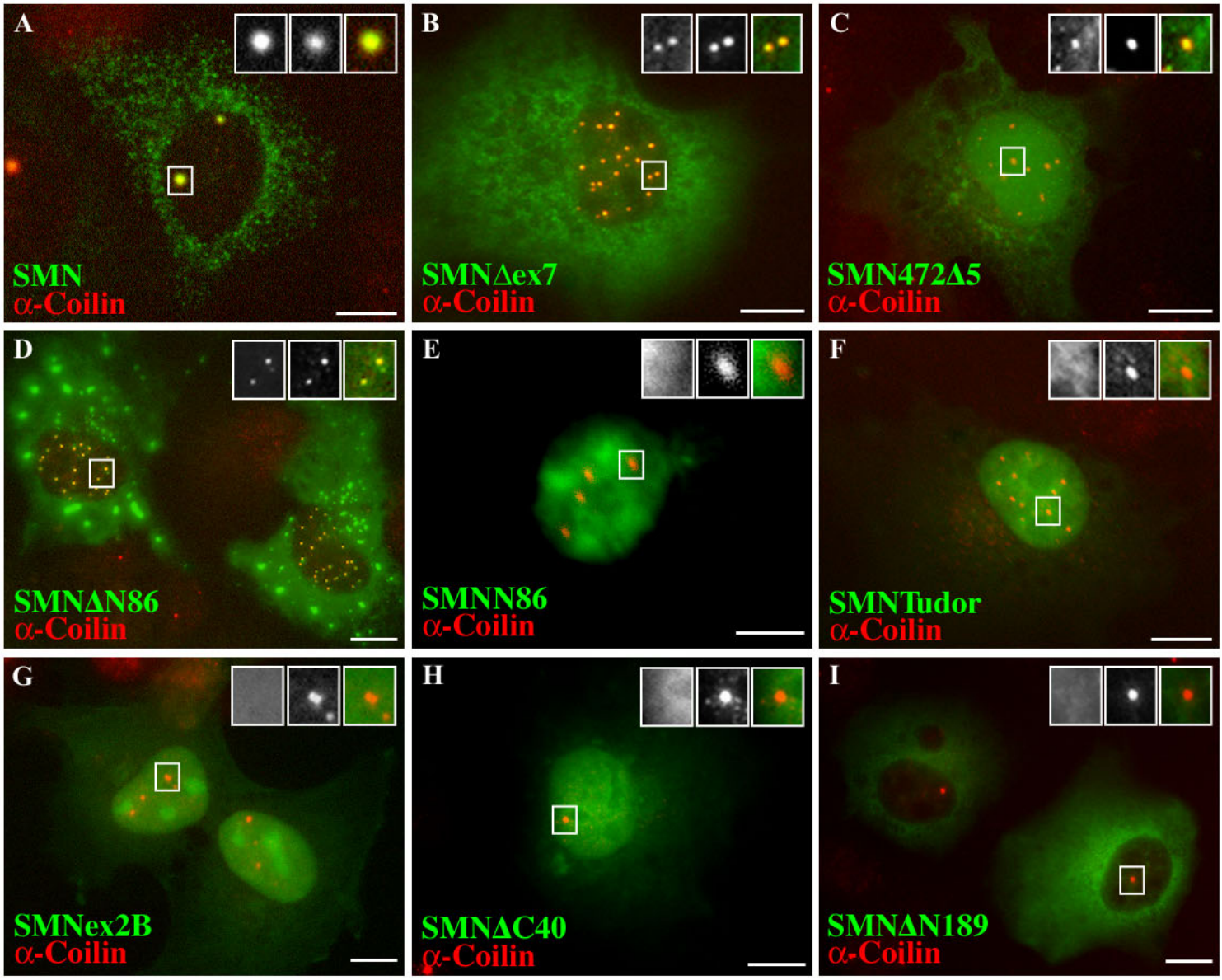
A
SMN
α-Coilin
B
SMNΔex7
α-Coilin
C
SMN472Δ5
α-Coilin
D
SMNΔN86
α-Coilin
E
SMNN86
α-Coilin
F
SMNTudor
α-Coilin
G
SMNex2B
α-Coilin
H
SMNΔC40
α-Coilin
I
SMNΔN189
α-Coilin

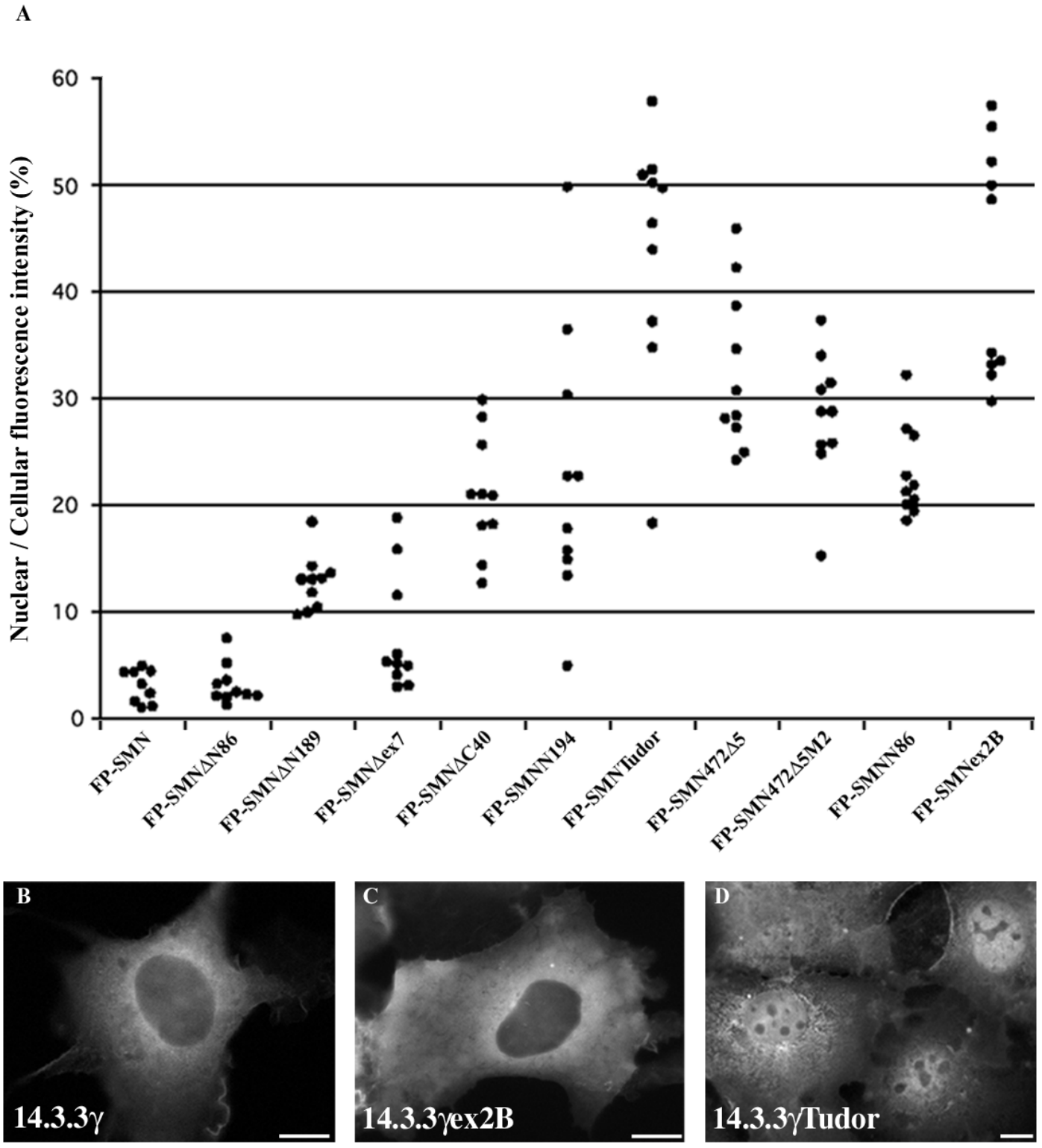
A
Nuclear / Cellular fluorescence intensity (%)
60
50
40
30
20
10
0
FP-SMN
FP-SMNΔN86
FP-SMNΔN189
FP-SMNΔex7
FP-SMNΔC40
FP-SMNN194
FP-SMNTudor
FP-SMN472Δ5
FP-SMN472Δ5M2
FP-SMNN86
FP-SMNex2B
B
14.3.3γ
C
14.3.3γex2B
D
14.3.3γTudor

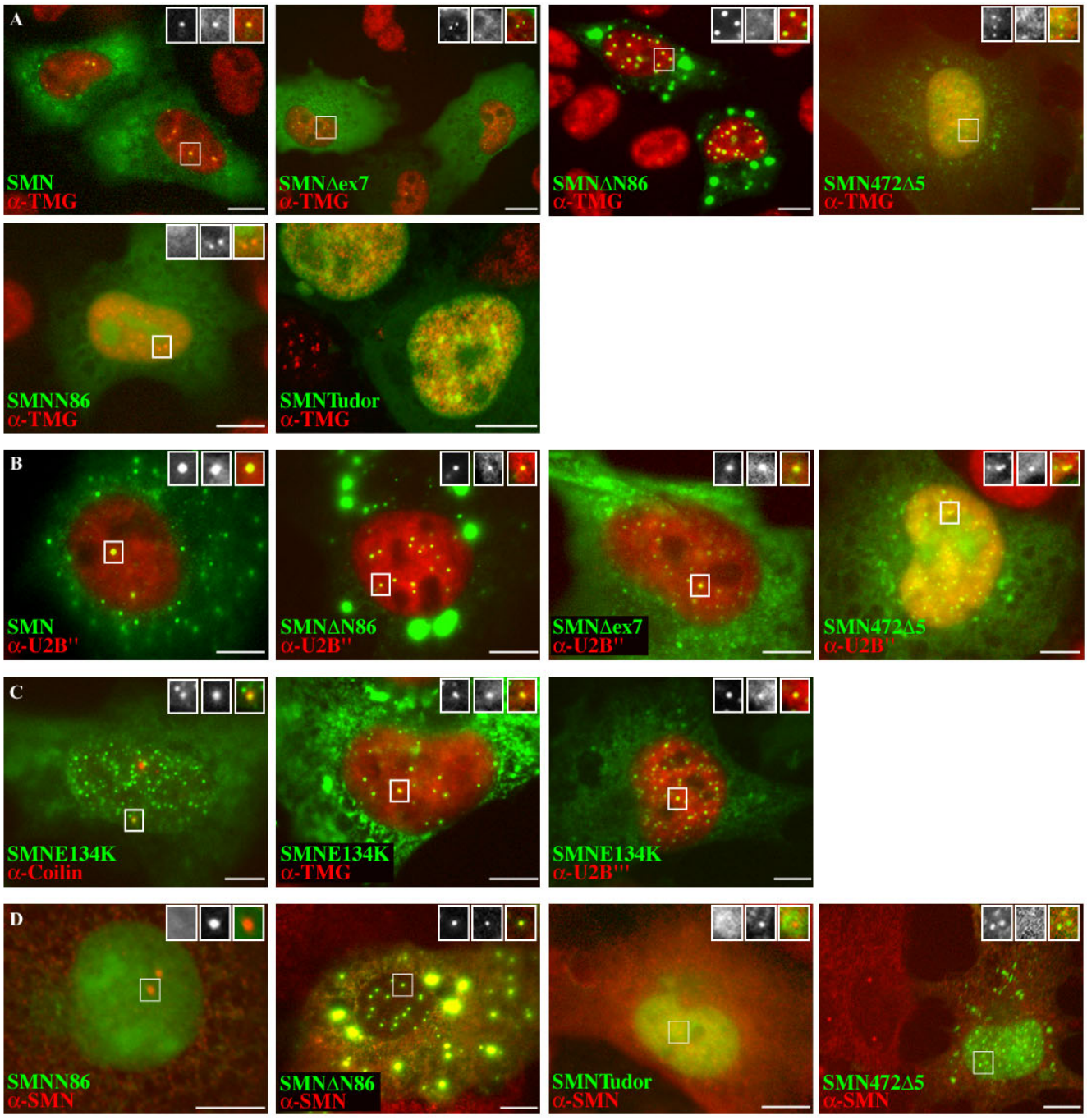
A
SMN
α-TMG
SMNΔex7
α-TMG
SMNΔN86
α-TMG
SMN472Δ5
α-TMG
SMNN86
α-TMG
SMNTudor
α-TMG
B
SMN
α-U2B''
SMNΔN86
α-U2B''
SMNΔex7
α-U2B''
SMN472Δ5
α-U2B''
C
SMNE134K
α-Coilin
SMNE134K
α-TMG
SMNE134K
α-U2B'''
D
SMNN86
α-SMN
SMNΔN86
α-SMN
SMNTudor
α-SMN
SMN472Δ5
α-SMN

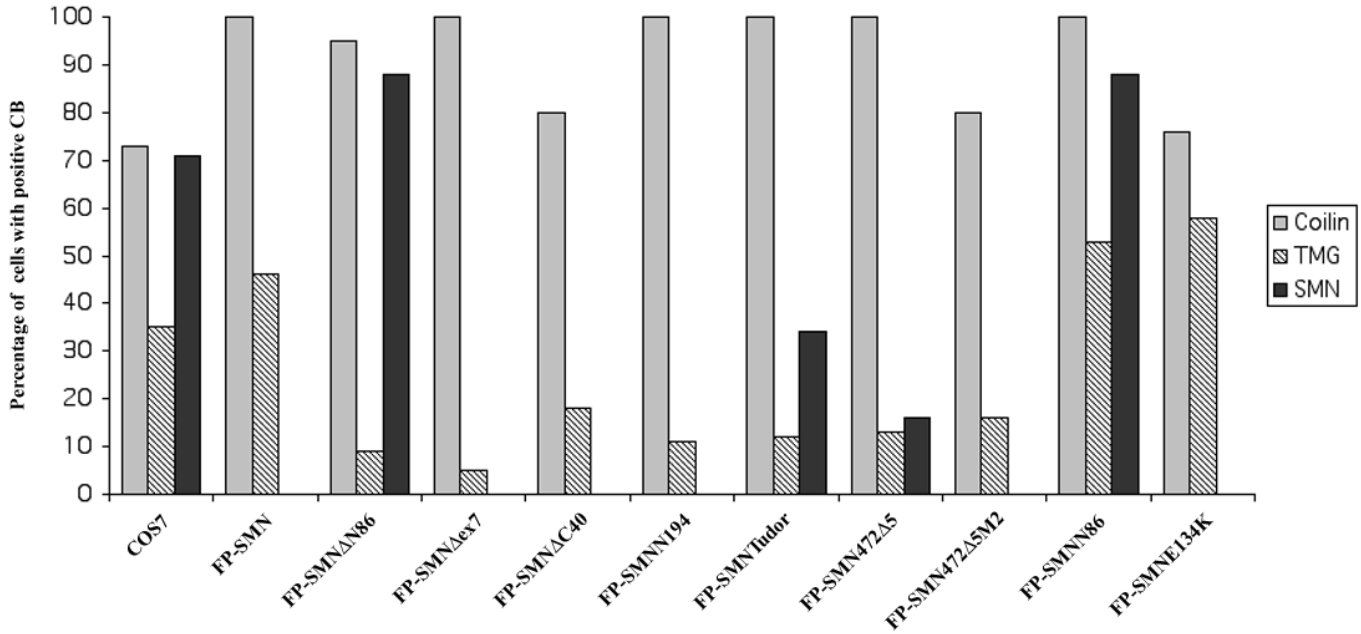
Percentage of cells with positive CB
100
90
80
70
60
50
40
30
20
10
0
Coilin
TMG
SMN
COS7
FP-SMN
FP-SMNΔN86
FP-SMNΔex7
FP-SMNΔC40
FP-SMNN194
FP-SMNTudor
FP-SMN472Δ5
FP-SMN472Δ5M2
FP-SMNN86
FP-SMNE134K

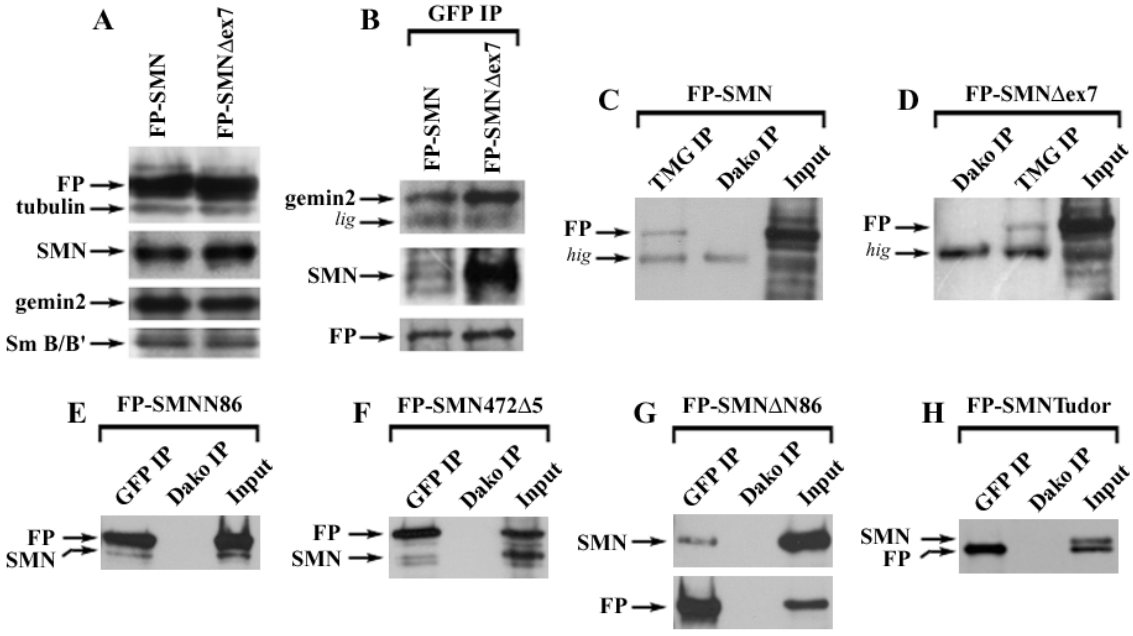
A
FP-SMN
FP-SMNΔex7
FP
tubulin
SMN
gemin2
Sm B/B'
B
GFP IP
FP-SMN
FP-SMNΔex7
gemin2
lig
SMN
FP
C
FP-SMN
TMG IP
Dako IP
Input
FP
hig
D
FP-SMNΔex7
Dako IP
TMG IP
Input
FP
hig
E
FP-SMNN86
GFP IP
Dako IP
Input
FP
SMN
F
FP-SMN472Δ5
GFP IP
Dako IP
Input
FP
SMN
G
FP-SMNΔN86
GFP IP
Dako IP
Input
SMN
FP
H
FP-SMNTudor
GFP IP
Dako IP
Input
SMN
FP

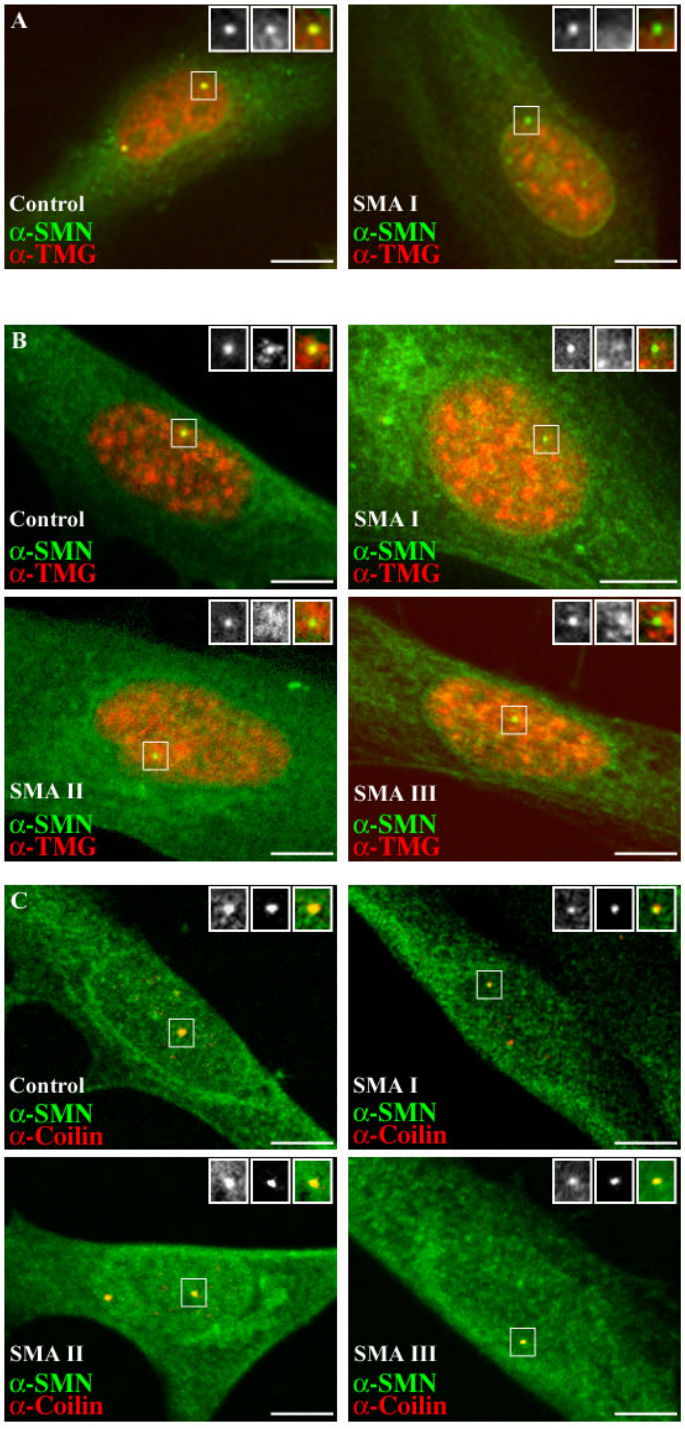
A
Control
α-SMN
α-TMG
SMA I
α-SMN
α-TMG
B
Control
α-SMN
α-TMG
SMA I
α-SMN
α-TMG
SMA II
α-SMN
α-TMG
SMA III
α-SMN
α-TMG
C
Control
α-SMN
α-Coilin
SMA I
α-SMN
α-Coilin
SMA II
α-SMN
α-Coilin
SMA III
α-SMN
α-Coilin

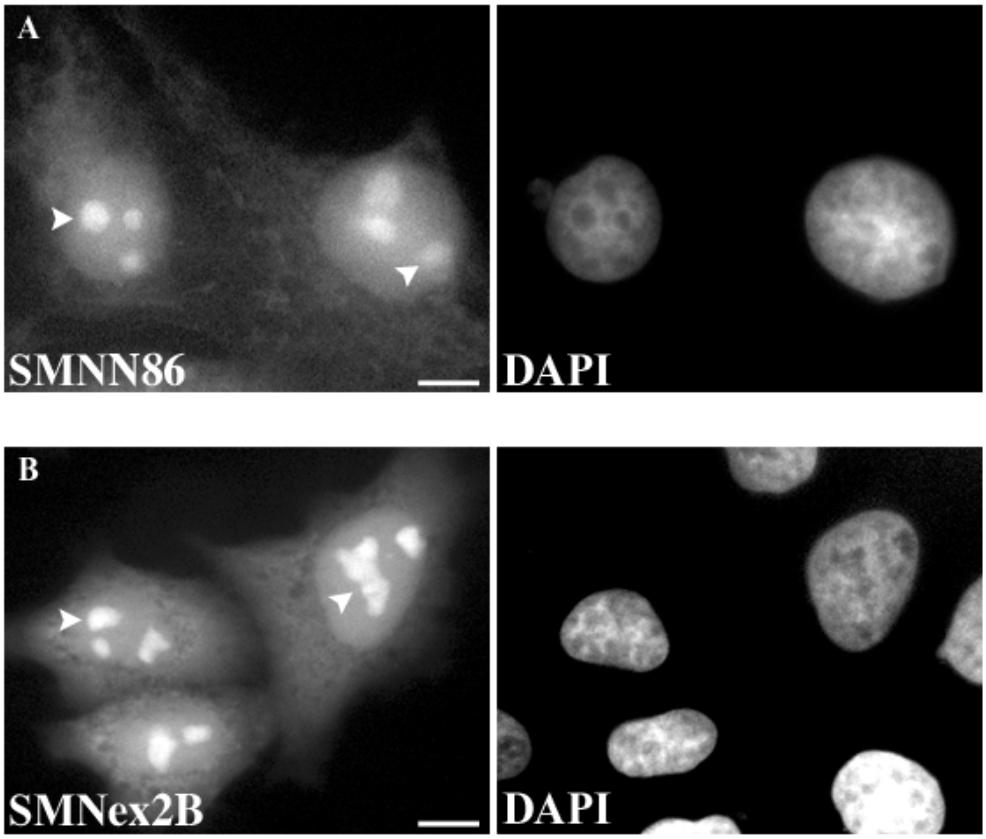
A
SMNN86
DAPI
B
SMNex2B
DAPI

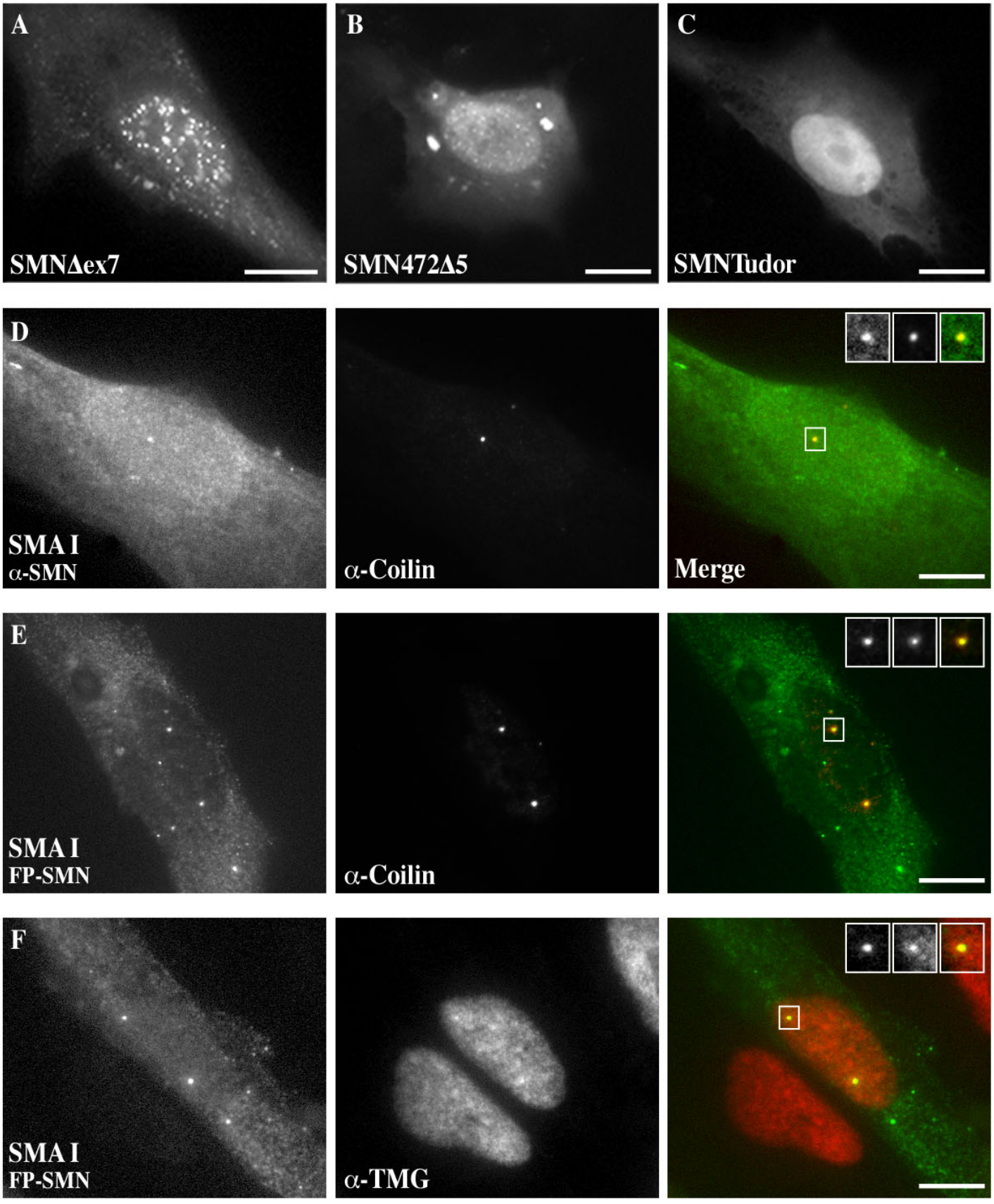
A
SMNΔex7
B
SMN472Δ5
C
SMNTudor
D
SMA I
α-SMN
α-Coilin
Merge
E
SMA I
FP-SMN
α-Coilin
F
SMA I
FP-SMN
α-TMG

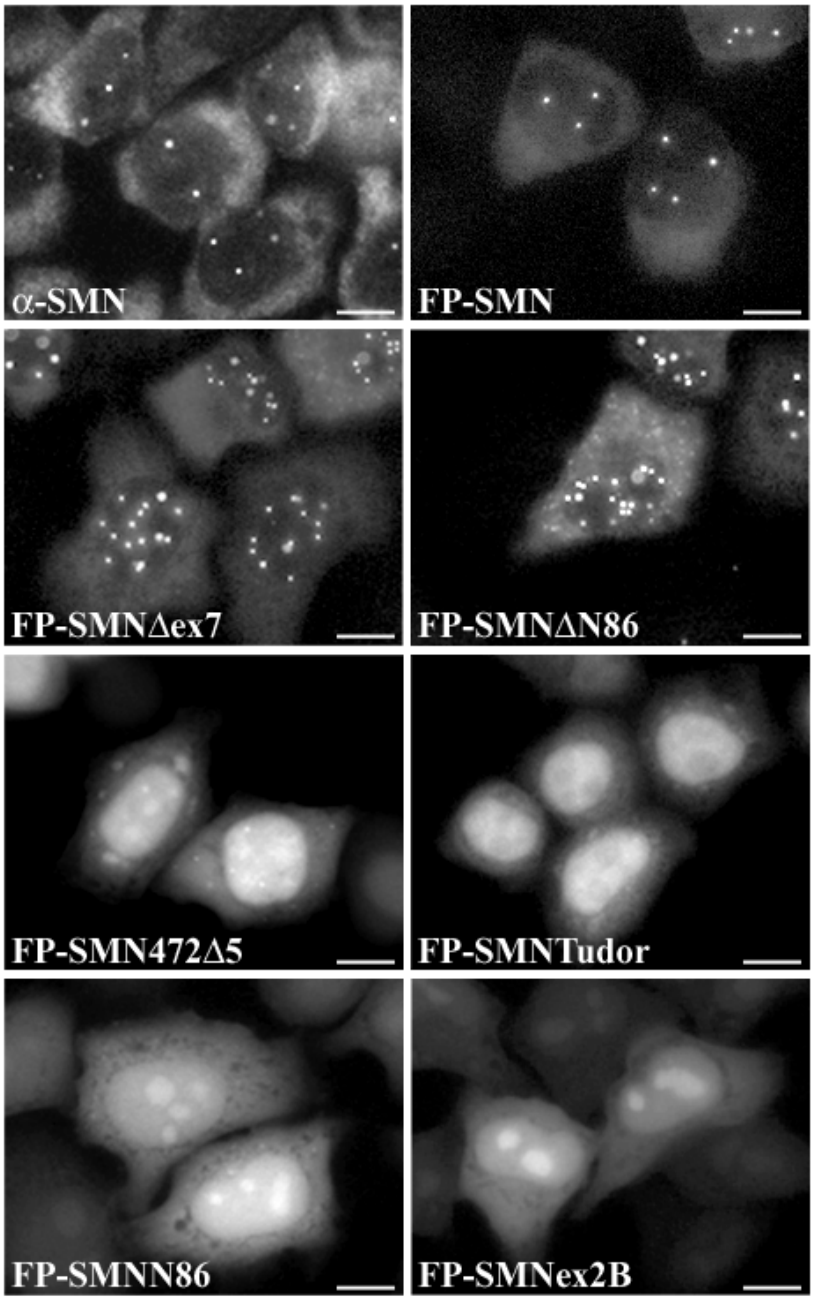
α-SMN
FP-SMN
FP-SMNΔex7
FP-SMNΔN86
FP-SMN472Δ5
FP-SMNTudor
FP-SMNN86
FP-SMNex2B